

Superconductivity in ultrasmall metallic grains

Fabian Braun and Jan von Delft

Institut für Theoretische Festkörperphysik, Universität Karlsruhe, D-76128 Karlsruhe, Germany

(Received 16 January 1998; revised manuscript received 27 April 1998)

Several recent papers have predicted parity effects, based on even-odd ground state energy differences, in ultrasmall (nm scale) superconductors having a discrete electronic eigenspectrum with mean level spacing $d \approx \tilde{\Delta}$ (bulk gap). The motivation for the present paper is to analyze the *measurability* of these and related parity effects in the present generation of experiments [e.g., those of Ralph, Black, and Tinkham (RBT)]. To this end we develop a general theory of superconductivity in ultrasmall metallic grains, based on calculating the eigenspectrum using a generalized BCS variational approach. We discuss how conventional mean field theory breaks down with decreasing sample size, how the so-called blocking effect weakens pairing correlations in states with nonzero total spin, and how this affects the discrete eigenspectrum's behavior in a magnetic field, which favors nonzero total spin. Our calculations qualitatively reproduce the magnetic-field-dependent tunneling spectra for individual aluminum grains measured by RBT. Our main results regarding parity effects are (i) the conclusion that those based on even-odd ground state energy differences are currently not measurable and (ii) the proposal of a parity effect for the pair-breaking energy, which should be measurable provided that the grain size can be controlled sufficiently well. [S0163-1829(99)07613-4]

I. INTRODUCTION

What happens to superconductivity when the sample is made very very small? Anderson¹ addressed this question already in 1959: he argued that if the sample is so small that its electronic eigenspectrum becomes discrete, with a mean level spacing $d = 1/N(\epsilon_F) \sim 1/\text{Vol}$, “superconductivity would no longer be possible” when d becomes larger than the bulk gap $\tilde{\Delta}$. Heuristically, this is obvious (see Fig. 1 below): $\tilde{\Delta}/d$ is the number of free-electron states that pair correlate (those with energies within $\tilde{\Delta}$ of ϵ_F), i.e., the “number of Cooper pairs” in the system; when this becomes ≤ 1 , it clearly no longer makes sense to call the system “superconducting.”

Giaever and Zeller^{2,3} were among the first to probe Anderson's criterion experimentally: studying tunneling through granular thin films containing electrically insulated Sn grains, they demonstrated the existence of an energy gap for grain sizes right down to the critical size estimated by Anderson (radii of 25 Å in this case), but were unable to prove that smaller particles are always normal. Their concluding comments are remarkably perspicuous:³ “There can be no doubt, however, that in this size region the bulk theory of superconductivity loses its meaning. As a matter of fact, perhaps we should not even regard the particles as metallic because the energy-level spacing is large compared to kT and because there are very few electrons at the Fermi surface. The question of the lower size limit for superconductivity is, therefore, strongly correlated with the definition of superconductivity itself.”

These remarks indicate succinctly why the study of superconductivity near its lower size limit is of fundamental interest: the conventional bulk BCS approach is not directly applicable, and some basic elements of the theory need to be rethought, with the role of level discreteness demanding special attention.

First steps in this direction were taken by Strongin *et al.*⁴ and by Mühlischlegel *et al.*,⁵ who calculated the thermody-

amic properties of small superconducting grains. However, since experiments at the time were limited to studying ensembles of small grains (e.g., granular films), there was no experimental incentive to develop a more detailed theory for an *individual* ultrasmall superconducting grain, whose eigenspectrum, for example, would be expected to reveal very directly the interplay between level discreteness and pairing correlations.

This changed dramatically in 1995, when Ralph, Black, and Tinkham (RBT) (Ref. 6) succeeded in constructing a single-electron transistor (SET) whose island was an ultrasmall metallic grain: by studying the tunneling current through the device, they achieved the first measurement of the discrete eigenspectrum of a single grain. This enabled them to probe the effects of spin-orbit scattering,^{7,8} nonequilibrium excitations,⁹ and superconductivity,^{7,9} which manifests itself through the presence (absence) of a substantial spectral gap in grains with an even (odd) number of electrons.

RBT's work stimulated several theoretical investigations. Besides discussing nonequilibrium effects,^{10,11} these focused mainly on superconductivity,¹²⁻¹⁶ and revealed that the breakdown of pairing correlations with decreasing grain size predicted by Anderson harbors some surprises when scrutinized in more detail: von Delft *et al.*¹² showed that this breakdown is affected by the *parity* (p) of the number of electrons on the grain: using parity-projected mean-field theory^{17,18} and variational methods and assuming uniformly spaced electron levels, they solved the parity-dependent gap equation for the even or odd ground state pairing parameters Δ_e or Δ_o as function of d (using methods adapted from Strongin *et al.*⁴), and found that $\Delta_o(d) < \Delta_e(d)$, i.e., ground state pairing correlations break down sooner with increasing d in an odd grain than in an even grain (the difference becoming significant for $d \approx \tilde{\Delta}$). This is due to the so-called *blocking effect*:¹⁹ the odd grain always has one unpaired electron, which blocks pair scattering of other pairs and

thereby weakens pairing correlations. Smith and Ambegaokar¹³ showed that this parity effect holds also for a random distribution of level spacings (as also anticipated by Blanter²⁰), and Matveev and Larkin¹⁴ investigated a ground state parity effect occurring in the limit $d \gg \bar{\Delta}$. Though stimulated by experiments neither of the theoretical works on parity effects did analyze their measurability in detail.

The $\Delta_o < \Delta_e$ parity effect has an obvious generalization, studied by Braun *et al.*¹⁵ using a generalized BCS variational approach due to Soloviev:¹⁹ any state with nonzero spin s (not just the odd ground state) experiences a significant reduction in pairing correlations, since at least $2s$ electrons are unpaired, leading to an enhanced blocking effect ($\Delta_s < \Delta_{s'}$ if $s > s'$). The latter's consequences can be observed in the magnetic-field dependence of SET tunneling spectra, since a magnetic field favors states with nonzero spin and consequent enhanced blocking effect. In ultrasmall grains, spin magnetism dominates orbital magnetism, just as in thin films in a parallel field;²¹ but whereas in the latter the magnetic-field induced transition to a normal state is known to be first order, Braun *et al.* showed that in ultrasmall grains the transition is softened due to finite size effects. Moreover, they argued that some of RBT's grains fall in a region of "minimal superconductivity," in which pairing correlations measurably exist at $H=0$, but are so weak that they may be destroyed by the breaking of a single pair (since the number of electron pairs that take part in the formation of a correlated state becomes of order one for $d \approx \bar{\Delta}$).

In the present paper we elaborate the methods used and results found by Braun *et al.* in Ref. 15 and present a detailed theory of superconductivity in ultrasmall grains. Our discussion can be divided into two parts: in the first (Secs. II and III), we consider an isolated ultrasmall grain and (a) define when and in what sense it can be called "superconducting," (b) use a generalized BCS variational approach to calculate the eigenenergies of various variational eigenstates of general spin $|s\rangle$, which illustrates the breakdown of mean-field theory, and (c) discuss how an increasing magnetic field induces a transition to a normal paramagnetic state. In the second part (Sec. IV), we consider the grain coupled to leads as in RBT's SET experiments and discuss observable quantities: (a) We calculate theoretical tunneling spectra of the RBT type, finding qualitative agreement with RBT's measurements, (b) *show that the above-mentioned ground state energy parity effects can presently not be observed, and propose an analogous pair-breaking energy parity effect that should be observable in experiments of the present kind.* In three appendixes we discuss various analytical limits of our theory, the general I - V characteristics expected for an ultrasmall NSN SET, and explain how RBT's experiments give direct evidence for the dominance of time-reversed pairing, at least for small fields (implying that the sufficiency of using only a reduced BCS Hamiltonian, well established for bulk systems and dirty superconductors, holds for ultrasmall grains, too).

II. PAIRING CORRELATIONS AT FIXED PARTICLE NUMBER

The discrete energies measured in RBT's experiments essentially correspond to the eigenspectrum of a grain with

fixed electron number N (for reasons explained in detail in Sec. IV A). In this and the next section, we therefore consider an ultrasmall grain *completely isolated* from the rest of the world, e.g., by infinitely thick oxide barriers.

When considering a truly isolated superconductor (another example would be a superconductor levitating in a magnetic field due to the Meissner effect) one needs to address the question: How is one to incorporate the fixed- N condition into BCS theory, and how important is it to do so? Although this issue is well understood and was discussed at length in the early days of BCS theory, in particular in its application to pairing correlations in nuclei (see Ref. 22, p. 439), for pedagogical reasons the arguments are worth recapitulating in the present context. We shall first recall that the notion of pair mixing¹² that lies at the heart of BCS theory is by no means inherently grand canonical and can easily be formulated in canonical language, then summarize what has been learned in nuclear physics about fixed- N projection techniques, and finally conclude that for present purposes, standard grand-canonical BCS theory should be sufficient. Readers familiar with the relevant arguments may prefer to skip this section.

A. Canonical description of pair mixing

Conventional BCS theory gives a grand-canonical description of the pairing correlations induced by the presence of an attractive pairing interaction such as the reduced BCS interaction

$$H_{\text{red}} = - \sum_{jj'} V c_{j+}^\dagger c_{j-}^\dagger c_{j'-} c_{j'+} \quad (\text{with } V > 0). \quad (1)$$

(The $c_{j\pm}$ are electron destruction operators for the single-particle states $|j, \pm\rangle$, taken to be time-reversed copies of each other, with energies $\epsilon_{j\pm}$.) The theory employs a grand-canonical ensemble, formulated on a Fock space of states in which the total particle number N is not fixed, as illustrated by BCS's variational ground state *Ansatz*

$$|\text{BCS}\rangle = \prod_j (u_j + v_j c_{j+}^\dagger c_{j-}^\dagger) |\text{Vac}\rangle \quad (u_j^2 + v_j^2 = 1). \quad (2)$$

This is not an eigenstate of the number operator $\hat{N} = \sum_{j\sigma} c_{j\sigma}^\dagger c_{j\sigma}$ and its particle number is fixed only on the average by the condition $\langle \text{BCS} | \hat{N} | \text{BCS} \rangle = N$, which determines the grand-canonical chemical potential μ . Likewise, the commonly used definition

$$\Delta_{\text{BCS}} = V \sum_j \langle c_{j+} c_{j-} \rangle \quad (3)$$

for the superconducting order parameter only makes sense in a grand-canonical ensemble, since it would trivially give zero when evaluated in a canonical ensemble, formulated on a strictly fixed- N Hilbert space of states.

A theory of strictly fixed- N superconductivity must therefore entail modifications of conventional BCS theory. In particular, a construction different from Δ_{BCS} is needed for the order parameter, which we shall henceforth call "pairing parameter," since "order parameter" carries the connotation of a phase transition, which would require the thermody-

dynamic limit $N \rightarrow \infty$. The pairing parameter should capture in a canonical framework BCS's essential insight about the nature of the superconducting ground state: an attractive pairing interaction such as H_{red} will induce pairing correlations in the ground state that involve *pair mixing* across ε_F (see also Ref. 12), i.e., a nonzero amplitude to find a pair of time-reversed states occupied above ε_F or empty below ε_F . BCS chose to express this insight through the *Ansatz* (2), which allows $v_j \neq 0$ for $\varepsilon_j > \varepsilon_F$ and $u_j \neq 0$ for $\varepsilon_j < \varepsilon_F$. It should be appreciated, however (and is made clear on p. 1180 of their original paper²³), that they chose a *grand-canonical* construction purely for calculational convenience (the trick of using commuting products in Eq. (2) makes it brilliantly easy to determine the variational parameters u_j, v_j), and proposed themselves to use its projection to fixed N , $|\text{BCS}\rangle_N$, as the actual ground state.

Since $[H_{\text{red}}, \hat{N}] = 0$, one would expect that the essence of BCS theory, namely, the presence of pair mixing and the reason why it occurs, can also be formulated in a canonically meaningful way. Indeed, this is easy: pair mixing is present if the amplitude $\bar{v}_j \equiv \langle c_{j+}^\dagger c_{j-}^\dagger c_{j-} c_{j+} \rangle^{1/2}$ to find a pair of states occupied is nonzero also for $\varepsilon_j > \varepsilon_F$, and the amplitude $\bar{u}_j \equiv \langle c_{j-} c_{j+} c_{j+}^\dagger c_{j-}^\dagger \rangle^{1/2}$ to find a pair of states empty is nonzero also for $\varepsilon_j < \varepsilon_F$ (the bars indicate that the \bar{u}_j and \bar{v}_j defined here differ in general from the u_j and v_j used by BCS; note, though, that the former reduce to the latter if evaluated using $|\text{BCS}\rangle$). The intuitive reason why H_{red} induces pair mixing in the exact ground states $|G\rangle$ despite the kinetic energy cost incurred by shifting pairing amplitude from below to above ε_F , is that this frees up phase space for pair-scattering, thus lowering the ground state expectation value of H_{red} : in $\langle G | H_{\text{red}} | G \rangle$, the jj' term can be nonzero only if both $c_{j+}^\dagger c_{j-}^\dagger c_{j'-} c_{j'+} |G\rangle \neq 0$, implying $(\bar{v}_{j'})_G \neq 0$ and $(\bar{u}_j)_G \neq 0$, and also $\langle G | c_{j+}^\dagger c_{j-}^\dagger c_{j'-} c_{j'+} \neq 0$, implying $(\bar{v}_j)_G \neq 0$ and $(\bar{u}_{j'})_G \neq 0$. By pair mixing, the system can arrange for a significant number of states to simultaneously have both $(\bar{v}_j)_G \neq 0$ and $(\bar{u}_j)_G \neq 0$; this turns out to lower the ground state energy sufficiently through $\langle G | H_{\text{red}} | G \rangle$ that the kinetic energy cost of pair mixing is more than compensated. Furthermore, an excitation that disrupts pairing correlations in the ground state by “breaking up a pair” will cost a finite amount of energy by *blocking* pair scattering involving that pair. For example, the energy cost of having $|j+\rangle$ definitely occupied ($\bar{u}_j = 0$) and $|j-\rangle$ definitely empty ($\bar{v}_j = 0$) is

$$\varepsilon_j \left(1 - \langle G | \sum_{\sigma} c_{j\sigma}^\dagger c_{j\sigma} | G \rangle \right) + V \langle G | c_{j+}^\dagger c_{j-}^\dagger \sum_{j' \neq j} c_{j'-} c_{j'+} | G \rangle,$$

in which the restricted sum reflects the blocking of scattering involving the j th pair. When evaluated using $|\text{BCS}\rangle$, this quantity reduces to $\varepsilon_j (1 - 2v_j^2) + u_j v_j \Delta_{\text{BCS}} = [\varepsilon_j^2 + \Delta_{\text{BCS}}^2]^{1/2}$, which is the well-known quasiparticle energy of the state $\gamma_{j+}^\dagger |\text{BCS}\rangle$.

The above simple arguments illustrate that there is nothing inherently grand canonical about pair mixing. Indeed, at least two natural ways suggest themselves to measure its strength in a canonically meaningful way, using, for instance, the pairing parameter $\bar{\Delta} \equiv V \sum_j \bar{u}_j \bar{v}_j$ proposed in Ref. 12, or one proposed by Ralph²⁴:

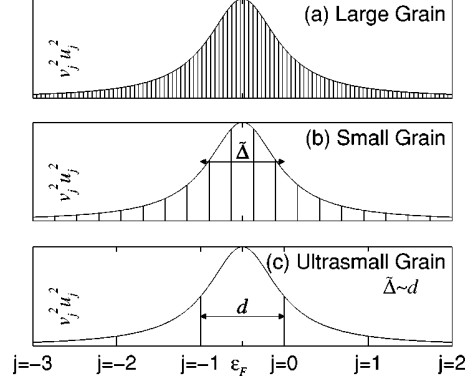


FIG. 1. An illustration of why “superconductivity breaks down” when the sample becomes sufficiently small. Each vertical line represents a pair of single-particle state $|j\pm\rangle$ with energy ε_j , for three different mean level spacings d , corresponding to (a) a “large” grain ($d \ll \bar{\Delta}$), (b) a “small” grain ($d \approx 0.25\bar{\Delta}$), (c) an “ultrasmall” grain ($d \approx \bar{\Delta}$). In all three plots, the height of each vertical line equals the function $u_j^2 v_j^2 = \frac{1}{4} [\bar{\Delta}^2 / (\varepsilon_j^2 + \bar{\Delta}^2)]$ of standard bulk BCS theory, illustrating the energy regime (of range $\bar{\Delta}$ around ε_F) within which electrons are affected by pairing correlations. Loosely speaking, the number of single-electron states $\bar{\Delta}/d$ in this regime corresponds to “the number of Cooper pairs” of the system. Evidently, when $d/\bar{\Delta} \geq 1$ as in (c), “the number of Cooper pairs” becomes less than one and it no longer makes sense to call the system “superconducting.”

$$\bar{\Delta}' \equiv V \sum_j [\langle c_{j+}^\dagger c_{j+} c_{j-}^\dagger c_{j-} \rangle - \langle c_{j+}^\dagger c_{j+} \rangle \langle c_{j-}^\dagger c_{j-} \rangle]^{1/2}. \quad (4)$$

Both $\bar{\Delta}$ and $\bar{\Delta}'$ were constructed such that they reduce, as is desirable, to the same result as Δ_{BCS} when each is evaluated using $|\text{BCS}\rangle$ (with real coefficients u_j, v_j), namely, to $V \sum_j u_j v_j$. An appealing feature of $\bar{\Delta}'$ is that by subtracting out $\langle c_{j+}^\dagger c_{j+} \rangle \langle c_{j-}^\dagger c_{j-} \rangle$, it transparently emphasizes the *pairing* nature of superconducting correlations, i.e., the fact that if $|j+\rangle$ is empty (or filled), so is $|j-\rangle$: $\bar{\Delta}'$ will be very small if the occupation of $|j+\rangle$ is uncorrelated with that of $|j-\rangle$, as it is in a normal Fermi liquid. The overall behavior (as function of energy ε_j) of the summands in both $\bar{\Delta}$ and $\bar{\Delta}'$ will be similar to that of $u_j v_j$ (though not identical to $u_j v_j$ or to each other; a quantitative evaluation of the differences, which increase with increasing $d/\bar{\Delta}$, requires an honest canonical calculation²⁵). The quantity $u_j v_j$ is shown in Fig. 1(a), which illustrates that pair-mixing correlations are strongest within a region of width Δ_{BCS} .

B. On the breaking of gauge symmetry

In some discussions of conventional BCS theory the defining feature of superconductivity is taken to be the breaking of gauge symmetry by the order parameter. This concept is illustrated by the BCS order parameter Δ_{BCS} of Eq. (3): if nonzero, it has a definite phase and is not gauge invariant (under $c_{j\sigma} \rightarrow e^{i\phi} c_{j\sigma}$, it changes to $e^{i2\phi} \Delta_{\text{BCS}}$). Note, though, that this point of view cannot be carried over to fixed- N systems. First, these trivially have $\Delta_{\text{BCS}} = 0$, and secondly

and more fundamentally, the breaking of gauge symmetry necessarily presupposes a grand-canonical ensemble: since phase and particle number are quantum-mechanically conjugate variables, formal considerations dictate that the order parameter can acquire a definite phase only if the particle number is allowed to fluctuate, i.e., in a grand-canonical ensemble.

Of course, in certain experimental situations where N manifestly *does* fluctuate, such as the celebrated Josephson effect of two superconductors connected by a tunnel junction, their order parameters *do* acquire definite phases, and their phase difference is a measurable quantity. However, for a truly isolated superconductor with fixed N the ‘‘phase of the order parameter’’ is *not* observable, and the concept of gauge symmetry breaking through an order parameter with a definite phase ceases to be useful. Indeed, the canonically meaningful pairing parameters $\bar{\Delta}$ and $\bar{\Delta}'$ defined above are manifestly gauge invariant.

C. Fixed- N projections

It is easy to construct a variational ground state exhibiting pair-mixing *and* having definite particle number, by simply projecting $|\text{BCS}\rangle$ to fixed N , as suggested by BCS.²³ This can be achieved by the projection integral

$$|\text{BCS}\rangle_N \equiv \int_0^{2\pi} d\phi e^{-i\phi N} \prod_j (u_j + e^{2i\phi} v_j c_{j+}^\dagger c_{j-}^\dagger) |\text{Vac}\rangle, \quad (5)$$

whose randomization of the phases of the v_j 's illustrates, incidentally, why gauge invariance is not broken at fixed N .

This and related fixed- N projections were studied in great detail in nuclear physics, with the aim of variationally calculating nuclear excitation spectra for finite nuclei ($N \leq 240$) exhibiting pairing correlations (Ring and Schuck provide an excellent review of the extensive literature, see chapter 11 of Ref. 22; Ref. 26 is a recent reference). The simplest approach is called ‘‘projection after variation’’: the unprojected expectation value $\langle \text{BCS} | H | \text{BCS} \rangle$ is minimized with respect to the variational parameters $\{v_j\}$, which thus have their standard BCS values $v_j^2 = \frac{1}{2} [1 - \epsilon_j / (\epsilon_j^2 + \Delta_{\text{BCS}}^2)^{1/2}]$, but then these are inserted into $|\text{BCS}\rangle_N$ and expectation values evaluated with the latter instead of $|\text{BCS}\rangle$. This elimination of ‘‘wrong- N ’’ states after variation turns out to lower the ground state energy relative to the unprojected case (by a few percent in nuclei) and thus improves the trial wave function. Further improvements are possible using the more sophisticated ‘‘projection before variation’’ strategy, where the projected expectation value ${}_N \langle \text{BCS} | H | \text{BCS} \rangle_N$ is minimized with respect to the $\{v_j\}$. However, these then no longer have the simple BCS form, but instead are determined through a set of *coupled* relations, each involving all the other v_j 's, that have to be solved numerically.²⁵ The corrections δv_j to the BCS pair-occupation amplitudes so produced further lower the ground state energy relative to projection after variation.

Extensive applications of such and related approaches in nuclear physics have led to the following conclusions: For reasonably small N , as in nuclei, the explicit implementation of projection techniques is tractable, though cumbersome. For very large N they become intractable, but also unneces-

sary, since their corrections can be shown to vanish as $N^{-1/2}$. However, even in nuclei the corrections to unprojected BCS theory are small (a few percent) in most cases, the only exception being very large couplings $V \geq d$. Thus, in most cases fixed- N systems can perfectly adequately be described by BCS's grand-canonical wave function. Its N indefiniteness (and the associated breaking of gauge symmetry) then simply has the status of a clever calculational trick: it allows the use of a wave function so simple that the pair-occupation amplitudes v_j can be found with a minimum of effort. The trick's justification is that the corrections δv_j 's produced by more careful approaches usually are small. (The device of using symmetry-breaking wave functions purely for the sake of calculational convenience is widespread in nuclear physics, and lucidly discussed in Ring and Schuck's book²² in a chapter entitled ‘‘Restoration of Broken Symmetries.’’)

The above conclusions imply that the following strategy should suffice for a *qualitative* description (more is not attempted here) of pairing correlations in isolated ultrasmall grains: although strictly speaking a fixed- N technique would be appropriate, we shall adopt BCS's grand-canonical approach throughout, using u_j, v_j as grand-canonical approximations to \bar{u}_j, \bar{v}_j . Quantitatively, this strategy is expected to become unreliable in the limit of large level spacing $d/\bar{\Delta} > 1$ (corresponding to ‘‘strong coupling’’ in nuclear applications). However, the corrections due to a fixed- N calculation (currently under investigation applying projection²⁵ and exact diagonalization²⁷ methods), which should become significant in this regime, are not expected to be more severe than, for example, corrections arising from a nonequidistant level spectrum, which qualitatively are insignificant.¹³

III. GENERALIZED VARIATIONAL BCS APPROACH

Since in RBT's experiments $T = 50 \text{ mK} \ll d, \bar{\Delta}$, we set $T = 0$. Our goal in this section is to calculate the discrete eigenenergies of an isolated, nm-scale metallic grain with pairing correlations, and understand their evolution in a magnetic field. To this end, we study the simplest conceivable pairing model within a generalized variational BCS approach. The results will be used in the next section as input into the calculation of the SET tunneling spectrum of such a grain (see Fig. 6 below).

A. The model

The only symmetry expected to hold in realistic, irregularly shaped ultrasmall grains at zero magnetic field is time-reversal symmetry. We therefore adopt a single-particle basis of pairs of time-reversed states $|j\pm\rangle$, whose discrete energies ϵ_j are assumed to already incorporate the effects of impurity scattering and the average of electron-electron interactions, etc. As simplest conceivable model describing a pairing interaction and a Zeeman coupling to a magnetic field, we adopt the following (reduced) BCS Hamiltonian:^{12,15}

$$\hat{H} = \sum_{j,\sigma=\pm} (\epsilon_j - \mu + \sigma h) c_{j\sigma}^\dagger c_{j\sigma} - \lambda d \sum_{j,j'} c_{j+}^\dagger c_{j-}^\dagger c_{j'-} c_{j'+}. \quad (6)$$

Due to level repulsion the ε_j 's will be approximately uniformly spaced. For simplicity, we take a completely uniform spectrum with *level spacing* d , $\varepsilon_j = jd + \varepsilon_0$. Fluctuations in the level spacings have been studied with methods of random matrix theory,¹⁵ with qualitatively similar results. For a system with a total of $N = 2m + p$ electrons, where the *electron number parity* p is 0 for even N and 1 for odd N , we use the label $j=0$ for the first level whose occupation in the $T=0$ Fermi sea is not 2 but p .

The pairing interaction is taken to include only states with $|dj| < \omega_c$. Experimental evidence for the sufficiency of neglecting couplings between non-time-reversed pairs of states, i.e., of using only a *reduced* BCS Hamiltonian, are given in Appendix C. For convenience we wrote the pair-coupling constant in Eq. (1) as $V = \lambda d$, where λ is a dimensionless parameter. The $d \rightarrow 0$ ‘‘bulk gap’’ of the model thus is $\tilde{\Delta} = \omega_c / \sinh(1/\lambda)$.

An applied magnetic field will completely penetrate an ultrasmall grain, since its radius (typically $r \approx 5$ nm) is much smaller than the penetration length of 50 nm for bulk Al. The Zeeman term in Eq. (6), with $\pm h \equiv \pm \frac{1}{2} \mu_B g H$, models the fact that the measured tunnel spectra of RBT (Refs. 7,9) (shown in Fig. 6 in Sec. IV B) evolve approximately linearly as a function of magnetic field, with g factors between 1.95 and 2 (determined from the differences between measured slopes of up- and down-moving lines). Deviations from $g = 2$ probably result from spin-orbit scattering, known to be small but nonzero in thin Al films,²¹ but neglected below (where $g = 2$ is used). Furthermore, orbital diamagnetism is also negligible, just as for thin films in a parallel magnetic field²¹ but in marked contrast to bulk samples where it causes the Meissner effect: the grains are so small that even a 7 T field produces a flux through the grain of only about 5% of a flux quantum ϕ_0 , which is too small to significantly affect the orbital motion of the electrons between subsequent reflections off the grain boundary. Some larger grains do show slight deviations from H -linearity,⁷ which probably reflect the onset of orbital magnetism [which gives corrections¹⁶ to the eigenenergies of the order of $\hbar v_F r^3 (H/\phi_0)^2$]; however, these effects are much smaller than Zeeman energies in the grains of present interest, and will be neglected here. Thus, our model assumes that Pauli paramagnetism due to the Zeeman energy completely dominates orbital diamagnetism, similarly to the case of thin films in parallel magnetic fields.²¹

B. The variational ansatz

The Zeeman term favors states with a nonzero total z component of the total spin $s = \sum_j s_j^z$ (henceforth simply called ‘‘spin’’), so that increasing h will eventually lead to a series of ground state changes to states with successively larger spins. Therefore, we are interested in general in correlated states with nonzero spin, and in particular in their eigenenergies. We calculate these variationally, using the following general *Ansatz* for a state $|s, \alpha\rangle$ with a definite total spin s (introduced by Soloviev for application in nuclei¹⁹):

$$|s, \alpha\rangle = \prod_{j=1}^{2s} c_{\alpha(j)}^\dagger \prod_i' (u_i^{(s, \alpha)} + v_i^{(s, \alpha)} c_{i+}^\dagger c_{i-}^\dagger) |\text{Vac}\rangle. \quad (7)$$

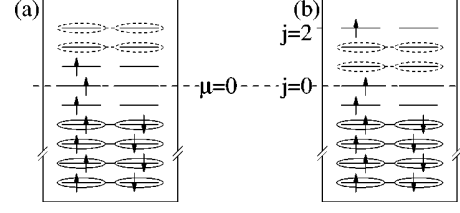


FIG. 2. Two examples of states in the spin- $\frac{3}{2}$ sector of Hilbert space: (a) the ground state $|\frac{3}{2}, 0\rangle$ and (b) the excited state $|\frac{3}{2}, 2\rangle$. The single-particle levels are drawn at $h=0$, and we indicated schematically how states are paired according to $(u_i + v_i c_{i+}^\dagger c_{i-}^\dagger)$ in the BCS-like *Ansätze* (15) and (17) for $|\frac{3}{2}, 0\rangle$ and $|\frac{3}{2}, 2\rangle$, with solid or dashed ellipses connecting states that would be completely filled or empty in the absence of pairing correlations.

The nonzero spin is achieved by placing $2s$ unpaired spin-up electrons in a set of $2s$ single particle states, say with labels $j = \alpha(1), \alpha(2), \dots, \alpha(2s)$ (see Fig. 2), while the remaining single-particle pairs of states have BCS-like amplitudes to be either filled ($v_i^{(s, \alpha)}$) or empty ($u_i^{(s, \alpha)}$), with $(u_i^{(s, \alpha)})^2 + (v_i^{(s, \alpha)})^2 = 1$. The prime over products (and over sums below) indicates exclusion of the singly occupied states $\alpha(1), \alpha(2), \dots, \alpha(2s)$ (for which $u^{(s, \alpha)}, v^{(s, \alpha)}$ are not defined).

A short standard calculation reveals that the constructed wave functions are orthogonal: $\langle s, \alpha | s', \alpha' \rangle = \delta_{ss'} \delta_{\alpha\alpha'}$. Therefore, the variational parameters $v_j^{(s, \alpha)}$ and $u_j^{(s, \alpha)}$ must be found *independently* for each (s, α) (hence the superscript). This is done by minimizing the variational ‘‘eigenenergies’’

$$\begin{aligned} \mathcal{E}_{s, \alpha}(h, d) \equiv \langle s, \alpha | H | s, \alpha \rangle &= -2sh + \sum_{j=1}^{2s} \varepsilon_{\alpha(j)} \\ &+ 2 \sum_j' \varepsilon_j (v_j^{(s, \alpha)})^2 - \lambda d \left(\sum_j' u_j^{(s, \alpha)} v_j^{(s, \alpha)} \right)^2 \\ &+ \lambda d \sum_j' (v_j^{(s, \alpha)})^4, \end{aligned} \quad (8)$$

which we use to approximate the model’s exact eigenenergies $E_{s, \alpha}(h, d)$. Note that singly occupied states are excluded from all primed sums involving u_j ’s and v_j ’s. The last term, proportional to v^4 , is not extensive and hence neglected in the bulk case where only effects proportional to the system volume are of interest. Here we retain it, since in ultrasmall systems it is non-negligible (but not dominant either).

Solving the energy-minimization conditions

$$\partial \mathcal{E}_{s, \alpha} / \partial v_j^{(s, \alpha)} = 0 \quad (9)$$

in standard BCS fashion yields

$$(v_j^{(s, \alpha)})^2 = (1 - \xi_j / [\xi_j^2 + \Delta_{s, \alpha}^2]^{1/2}) / 2, \quad (10)$$

where the ‘‘pairing parameter’’ $\Delta_{s, \alpha}$ is determined by the generalized ‘‘gap equation’’

$$\Delta_{s, \alpha} = \lambda d \sum_j' u_j^{(s, \alpha)} v_j^{(s, \alpha)} \quad \text{or} \quad (11)$$

$$\frac{1}{\lambda} = d \sum_j' \frac{1}{2\sqrt{\xi_j^2 + \Delta_{s,\alpha}^2}}, \quad (12)$$

and $\xi_j \equiv \varepsilon_j - \mu - \lambda d (v_j^{(s,\alpha)})^2$. Note that we retain the $\lambda d (v_j^{(s,\alpha)})^2$ shift in ξ_j , usually neglected because it simply renormalizes the bare energies, since for large d it somewhat increases the effective level spacing near ε_F [and its neglect turns out to produce a significant upward shift in the $\mathcal{E}_{s,\alpha}(h,d)$'s, which one is trying to minimize]. The chemical potential μ is fixed by requiring that

$$2m + p = \langle s, \alpha | \hat{N} | s, \alpha \rangle = 2s + 2 \sum_j' (v_j^{(s,\alpha)})^2. \quad (13)$$

Generally Eqs. (10), (12), and (13) have to be solved simultaneously numerically. In the limit $d/\tilde{\Delta} \rightarrow 0$ (investigated analytically in Appendix A 1), Eq. (12) reduces to the standard bulk $T=0$ gap equation.

In contrast to conventional BCS theory, the pairing parameter $\Delta_{s,\alpha}$ can in general not be interpreted as an energy gap and is *not* an observable. It should be viewed simply as a mathematical auxiliary quantity which was introduced to conveniently solve Eq. (9). However, by parametrizing the variational quantities $v_j^{(s,\alpha)}$ and $u_j^{(s,\alpha)}$, $\Delta_{s,\alpha}$ does serve as a measure of the pairing correlations present in a state $|s, \alpha\rangle$, since for vanishing $\Delta_{s,\alpha}$ the latter reduces to an uncorrelated paramagnetic state with spin s , namely,

$$|s, \alpha\rangle_0 \equiv \prod_{j=1}^{2s} c_{\alpha(j)+}^\dagger \prod_{i<0}' c_{i+}^\dagger c_{i-}^\dagger |0\rangle. \quad (14)$$

We shall denote the energy of this uncorrelated state by $\mathcal{E}_{s,\alpha}^0 = {}_0\langle s, \alpha | H | s, \alpha \rangle_0$, and define the ‘‘correlation energy’’ of $|s, \alpha\rangle$ as the energy difference $\mathcal{E}_{s,\alpha}^{\text{corr}} \equiv \mathcal{E}_{s,\alpha} - \mathcal{E}_{s,\alpha}^0$.

C. Qualitative discussion

Before launching into numerical results, let us anticipate by qualitative arguments what is to be expected.

First, the gap equation for $\Delta_{s,\alpha}(d)$ is h independent. The reason is that only those j levels contribute in the gap equation that involve correlated *pairs* of states, each of which have spin 0 and hence no Zeeman energy. Consequently, the $-2sh$ -dependence of $\mathcal{E}_{s,\alpha}$ in Eq. (8) is simply that of the $2s$ unpaired electrons.

Secondly, the discreteness of the sum in the gap equation (12) will cause $\Delta_{s,\alpha}$ to decrease with increasing d . To see this, inspect Fig. 1, in which the height of each vertical line represents the value of $u_j v_j$ for a time-reversed pair $|j \pm\rangle$. Figures 1(a)–1(c) illustrate that an increase in level spacing implies a decrease in the number of pairs with significant pair-mixing, i.e., those within $\tilde{\Delta}$ of ε_F which have nonzero $u_j v_j$. This number can roughly speaking be called the ‘‘number of Cooper pairs’’ of the system. Since for $d \gg \tilde{\Delta}$ no pairs lie in the correlated regime $|\varepsilon_j - \varepsilon_F| < \tilde{\Delta}$ where pair mixing occurs, $\Delta_{s,\alpha}$ will be zero in this limit, so that in general $\Delta_{s,\alpha}(d)$ will be a decreasing function of d , dropping to zero at about $d \approx \tilde{\Delta}$.

Thirdly, the (s, α) -dependent restriction on the primed sum in the gap equation implies that $\Delta_{s,\alpha}(d)$ at fixed d will

decrease with increasing s : larger s means more unpaired electrons, more terms missing from the primed sum, less correlated pairs and hence smaller $\Delta_{s,\alpha}$. The physics behind this has been called the *blocking effect*¹⁹ in nuclear physics: Singly occupied states cannot take part in the pair scattering caused by the BCS-like interaction (6) and hence decrease the phase space for pair scattering, as explained in Sec. II A. (Their absence in the primed sum simply reflects this fact.) The blocking effect becomes stronger with increasing d , since then the relative weight of each term missing in the primed sum increases. It also is stronger the closer the blocked state lies to ε_F , since the excluded $u_j^{(s,\alpha)} v_j^{(s,\alpha)}$ contribution to the primed sum is largest near ε_F , as is evident from Fig. 1. On the other hand, an unpaired electron will have almost no blocking effect if $|\varepsilon_j - \varepsilon_F| \gg \tilde{\Delta}$, since $u_j^{(s,\alpha)} v_j^{(s,\alpha)}$ vanishes there anyway.

Finally, note that the (s, α) dependence of $\Delta_{s,\alpha}$ for $d \approx \tilde{\Delta}$ illustrates why in this regime a conventional mean-field treatment is no longer sufficient: the system cannot be characterized by a single pairing parameter, since the amount of pairing correlations vary from state to state, each of which is characterized by its own pairing parameter.

D. General numerical solution

It is possible to solve the modified gap equation analytically in two limits, $d \ll \tilde{\Delta}$ and $d \gg \Delta_s$ (see Appendix A), but generally the gap equation and Eq. (13) have to be solved numerically. In doing so, some assumptions are necessary about parameter values (though using slightly different values would not change the results qualitatively). We measure all energies in units of the bulk gap $\tilde{\Delta} = \omega_c \sinh(1/\lambda)$ of the model. However, its experimental value differs from that of a truly bulk system, since it is known from work with Al thin films^{4,28} that the effective dimensionless pairing-interaction strength λ is larger in Al samples of reduced dimensionality than in truly bulk three-dimensional systems. (Though true for Al, this is not a universal property of small samples, though, for Nb, $\tilde{\Delta}$ is larger in the bulk than in thin films.²⁴) Since thin films in a parallel magnetic field are analogous in many ways to ultrasmall grains, we shall assume that the effective coupling constant λ is the same in both. Adopting, therefore, the value $\tilde{\Delta} = 0.38$ meV found for thin Al films in Ref. 29, and taking the cutoff to be the Debye frequency $\omega_c = 34$ meV of Al, we use $\lambda = [\sinh^{-1}(\omega_c/\tilde{\Delta})]^{-1} = 0.194$ for the dimensionless pairing-interaction strength. Furthermore, we smeared the cutoff of the BCS interaction over two single-electron levels, to ensure that discontinuities do not occur in d -dependent quantities each time the energy $|\varepsilon_j = dj + \varepsilon_0|$ of some large- $|j|$ level moves beyond the cutoff ω_c as d is increased.

Solving Eqs. (10), (12), and (13) is a straightforward numerical exercise which we performed, for the sake of ‘‘numerical consistency,’’ without further approximations. (Since some minor approximations were made in Ref. 15, e.g., dropping the $\lambda d v_j^2$ term in ξ_j , and slightly different parameter values were used, the numerical results there sometimes differ slightly from the present ones; see, e.g., Fig. 3.) It should be understood, though, that only qualitative significance can be attached to our numerical results, since

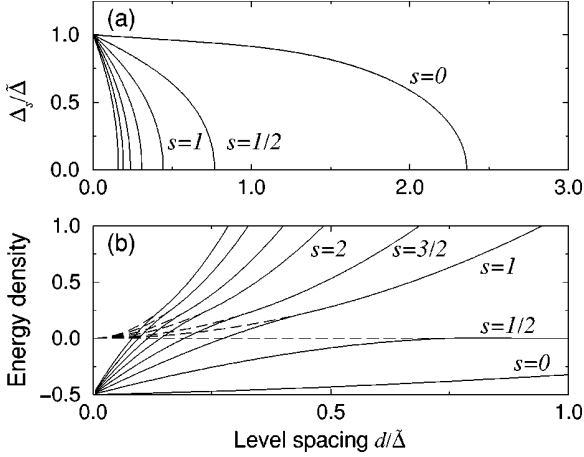


FIG. 3. Properties of spin- s ground states $|s\rangle$ [compare Eq. (15)]: (a) The pairing parameters $\Delta_s(d)/\bar{\Delta}$ for some spin- s ground states $|s\rangle$, as a function of $d/\bar{\Delta}$. The critical level spacings $d_{c,s}$ at which $\Delta_s(d_{c,s})=0$ are found to be 2.36, 0.77, 0.44, 0.31, \dots , for $s=0, 1/2, 1, 3/2, \dots$, respectively. (b) The energy densities $(\mathcal{E}_s - \mathcal{E}_{p/2}^0)/d\bar{\Delta}^2$ (solid lines), plotted as functions of $d/\bar{\Delta}$ for $h=0$, of some pair-correlated spin- s ground states $|s\rangle$ relative to the uncorrelated spin- $p/2$ Fermi sea $|p/2\rangle_0$, and for comparison the relative energy densities $(\mathcal{E}_s^0 - \mathcal{E}_{p/2}^0)/d\bar{\Delta}^2$ (dashed lines) of the corresponding uncorrelated paramagnetic states $|s\rangle_0$ (obtained from $|s\rangle$ by setting $\Delta_s=0$). We call the plotted quantities energy densities since the normalization factor $d/\bar{\Delta}^2$ contains $d \sim \text{Vol}^{-1}$. The solid and dashed spin- s lines meet at the critical level spacing $d_{c,s}$, above which no pairing correlations survive (so that the relative energy densities equal $[s^2 - p/4 + (s - p/2)\lambda]d^2/\bar{\Delta}^2$ there).

our model is very crude: it neglects, for instance, fluctuations in level spacing and in pair-coupling constants, and we do not carry out a fixed- N projection, all of which presumably would somewhat influence the results quantitatively.

1. Spin- s ground states

In a given spin- s sector of Hilbert space (with $p = 2s \bmod 2$), let $|s\rangle$ be the variational state with the lowest energy, i.e., the “variational spin- s ground state.” It is obtained by placing the $2s$ unpaired electrons as close as possible to ϵ_F [Fig. 2(a)], because this minimizes the kinetic energy cost of having more spin ups than downs:

$$|s\rangle = \prod_{j=-s+p/2}^{s-1+p/2} c_{j+}^\dagger \prod_i' (u_i^s + v_i^s c_{i+}^\dagger c_{i-}^\dagger) |\text{Vac}\rangle. \quad (15)$$

[The particular choice of α in the general Ansatz (7) to which $|s\rangle$ corresponds is $\alpha(n) = n - [s] - 1$ for $n = 1 \dots 2s$, where $[s]$ is the largest integer $\leq s$.] The numerical results for the corresponding pairing parameters $\Delta_s(d)$, shown in Fig. 3(a) for some several small s , confirm the properties anticipated in the previous subsection’s qualitative discussion.

First, each Δ_s decreases with d , vanishing at a critical level spacing $d_{c,s}$ beyond which no pair-mixing correlations exist in this level of approximation. In Appendix A 2 it is shown that near $d_{c,s}$, $\Delta_s(d)$ has the standard mean-field form $\sqrt{1 - d/d_{c,s}}$; this was to be expected, since the variational approach to finding $|s\rangle$ is equivalent to doing standard

mean-field theory within the spin- s sector of Hilbert space. (Note that one should not attach too much significance to the precise numerical values of the $d_{c,s}$ reported in Fig. 3, since they depend sensitively on model assumptions: for example, the values for $d_{c,0}$ and $d_{c,1/2}$ differ somewhat from those reported in Refs. 12 and 15, due to their use of a slightly different λ and minor numerical approximations not used here, as mentioned above. Moreover, Smith and Ambegaokar¹³ showed that the precise distribution of levels used influences $d_{c,s}$ significantly.)

Secondly, Δ_s decreases rapidly with increasing s at fixed d (and $d_{c,s} < d_{c,s'}$ if $s > s'$), illustrating the blocking effect. This result, which is expected to be independent of model details, is a generalization of the parity effect discussed by von Delft *et al.*¹² [They studied only ground state pairing correlations and found that these are weaker in odd ($s = 1/2$) grains than in even ($s = 0$) grains, $\Delta_{\text{odd}} = \Delta_{1/2} < \Delta_{\text{even}} = \Delta_0$.] The blocking effect is most dramatic in the regime $d/\bar{\Delta} \in [0.77, 2.36]$ in which $\Delta_0 \neq 0$ but $\Delta_{s \neq 0} = 0$. This is a regime of “minimal superconductivity,”¹⁵ in the sense that all pairing correlations that still exist in the even ground state (since $\Delta_0 \neq 0$) are completely destroyed by the addition of a single electron or the flipping of a single spin (since $\Delta_{s \neq 0} = 0$).

Figure 3(b) shows the eigenenergies \mathcal{E}_s (solid lines) of $|s\rangle$ and the energies \mathcal{E}_s^0 (dotted lines) of the corresponding uncorrelated paramagnetic states

$$|s\rangle_0 = \prod_{j=-s+p/2}^{s-1+p/2} c_{j+}^\dagger \prod_{i < -s+p/2} c_{i+}^\dagger c_{i-}^\dagger |\text{Vac}\rangle. \quad (16)$$

The solid and dashed spin- s lines meet at the critical level spacing $d_{c,s}$, above which no pairing correlations survive.

2. Spin- s excited states

Among all possible excited states with definite s , we consider here only those created from $|s\rangle$ by exciting one electron from the topmost occupied level $s - 1 + p/2$ of $|s\rangle$ to some higher level $j + s - 1 + p/2$:

$$|s, j\rangle = c_{(j+s-1+p/2)+}^\dagger \prod_{j=-s+p/2}^{s-2+p/2} c_{j+}^\dagger \times \prod_i' (u_i^s + v_i^s c_{i+}^\dagger c_{i-}^\dagger) |\text{Vac}\rangle. \quad (17)$$

[This reduces to $|s\rangle$ if $j=0$; the particular choice of α in Ansatz (7) to which $|s, j\rangle$ corresponds is $\alpha(n) = n - [s] - 1$ for $n = 1 \dots 2s - 1$ and $\alpha(2s) = [s] - 1 + j$.]

Interestingly, one finds that the larger j , the longer the pairing correlations survive with increasing d . This is illustrated by the simple example $s = 1/2$: Fig. 4(a) shows that the critical spacings $d_{c,1/2,j}$ [at which the pairing parameters $\Delta_{1/2,j}(d)$ vanish] increase with j , approaching the value $d_{c,0}$ of the spin-0 case as $j \rightarrow \infty$. This result is reflected in the excitation energies of Fig. 4(b): the excited states of the spin-1/2 sector have nonzero correlation energies (difference between solid and dashed lines) at d values for which the spin-1/2 ground state correlation energy of Fig. 3(b) is already zero. The intuitive reason why more highly excited

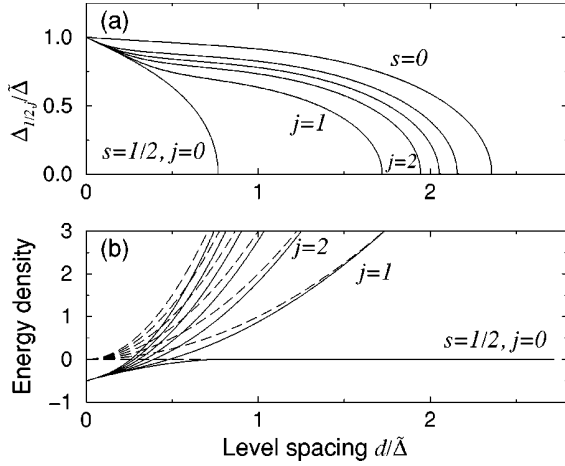


FIG. 4. Properties of excited spin- $\frac{1}{2}$ states $|\frac{1}{2}, j\rangle$ [compare Eq. (17)]: (a) The pairing parameter $\Delta_{1/2,j}$ for some spin- $\frac{1}{2}$ states $|\frac{1}{2}, j\rangle$ ($j=0, \dots, 4$), together with Δ_0 of the spin-0 ground state $|0\rangle$ (the outermost curve). The larger j , the closer $\Delta_{1/2,j}$ approaches the spin-0 value Δ_0 . (b) The relative energy densities $(\mathcal{E}_{1/2,j} - \mathcal{E}_{1/2,0}^0)d/\tilde{\Delta}^2$ (solid lines) of $|\frac{1}{2}, j\rangle$ relative to $|\frac{1}{2}, 0\rangle = |\frac{1}{2}\rangle_0$, and for comparison the relative energy densities $(\mathcal{E}_{1/2,j}^0 - \mathcal{E}_{1/2,0}^0)d/\tilde{\Delta}^2$ (dashed lines) of the corresponding uncorrelated state $|\frac{1}{2}, j\rangle_0$. For excited states the solid and dashed lines meet at a larger d than for the ground state, i.e., in excited states pairing correlations survive down to smaller grain sizes than in the corresponding ground state.

states have more pairing correlations than the corresponding spin-1/2 ground state $|\frac{1}{2}\rangle$ is of course quite simple: The larger j , i.e., the further the unpaired electron sits from the Fermi surface where pairing correlations are strongest, the less it disrupts pair mixing (since $u_j v_j$ becomes very small for large j , see Fig. 1). In fact, for very large j , the state $|\frac{1}{2}, j\rangle$ will have just about the same amount of pairing correlations as the even ground state $|0\rangle$ ($\Delta_{1/2,j} \approx \Delta_0$), since the unpaired electron sits so far from ε_F that the pairing correlations are effectively identical to those of $|0\rangle$.

Similar effects are seen for excited states in other spin sectors $s \neq \frac{1}{2}$. The higher the excitation, the larger the pairing parameter $\Delta_{s,\alpha}$. Nevertheless the energy of the excited states is always higher than that of the corresponding spin- s ground state, since the kinetic-energy cost of having an unpaired electron far from ε_F can be shown to always outweigh the interaction-energy gain due to having less blocking and hence a larger $\Delta_{s,\alpha}$.

E. Magnetic field behavior

In a magnetic field, the Zeeman energy favors states with nonzero spin. However, since such states have smaller correlation energy due to the blocking effect a competition arises between Zeeman energy and correlation energy. The manifestations of the blocking effect can thus be probed by turning on a magnetic field; if it becomes large enough to enforce a large spin, excessive blocking will destroy all pairing correlations.

The situation is analogous to ultrathin films in a parallel magnetic field,²¹ where orbital diamagnetism is negligible for geometrical reasons and superconductivity is destroyed at

sufficiently large h by Pauli paramagnetism. This occurs via a first order transition to a paramagnetic state, as predicted by Clogston and Chandrasekhar (CC) (Refs. 30,31) by the following argument (for bulk systems): A pure Pauli paramagnet has ground state energy $-h^2 \mathcal{N}(\varepsilon_F)$ and spin $s = h \mathcal{N}(\varepsilon_F)$ [since it chooses its spin such that the sum of the kinetic and Zeeman energies at spin s , $s^2 \mathcal{N}(\varepsilon_F) - 2hs$, is minimized]. When this energy drops below the bulk correlation energy $-\frac{1}{2} \tilde{\Delta}^2 \mathcal{N}(\varepsilon_F)$ of the superconducting ground state, which happens at the critical field $h_{CC} = \tilde{\Delta}/\sqrt{2}$, a transition will occur from the superconducting to the paramagnetic ground state. The transition is first order, since the change in spin, from 0 to $s_{CC} = h_{CC} \mathcal{N}(\varepsilon_F) = \tilde{\Delta}/(d\sqrt{2})$, is macroscopically large [$\mathcal{N}(\varepsilon_F) = 1/d \approx \text{Vol}$]. In tunneling experiments into ultrathin (5 nm) Al films ($\tilde{\Delta} = 0.38$ meV and $H_{CC} = 4.7$ T) this transition has been observed²⁹ as a jump in the tunneling threshold (from $\tilde{\Delta} - h_{CC}$ to zero) at h_{CC} .

In isolated ultrasmall grains, the above picture of the transition needs to be rethought in two respects due to the discreteness of the electronic spectrum: First, the spin must be treated as a discrete (instead of continuous) variable, whose changes with increasing h can only take on (parity conserving) integer values. Secondly, one needs to consider more carefully the possibility of h -induced transitions to nonzero spin states that are still *pair correlated* (instead of being purely paramagnetic), such as the variational states $|s, \alpha\rangle$ discussed above. (In the bulk case, it is obvious that such states play no role: the lowest pair-correlated state with nonzero spin obtainable from the ground state by spin flips is a two-quasiparticle state, costing energy $2\tilde{\Delta} - 2h$; when h is increased from 0, the paramagnetic transition at $h_{CC} = \tilde{\Delta}/\sqrt{2}$ thus occurs before a transition to this state, which would require $h = \tilde{\Delta}$, can occur.)

Within our variational approach, the effect of increasing h from 0 can be analyzed as follows: At given d and h , the grain's ground state is the lowest-energy state among all possible spin- s ground states $|s\rangle$ having the correct parity $2s \bmod 2 = p$. Since $\mathcal{E}_s(h, d) = \mathcal{E}_s(0, d) - 2hs$, level crossings occur with increasing h , with $\mathcal{E}_{s'}$ dropping below \mathcal{E}_s at the *level crossing field*

$$h_{s,s'}(d) = \frac{\mathcal{E}_{s'}(0, d) - \mathcal{E}_s(0, d)}{2(s' - s)}. \quad (19)$$

Therefore, as h is slowly turned on from zero with initial ground state $|s_0 = p/2\rangle$, a cascade of successive ground-state changes (GSC's) to new ground states $|s_1\rangle, |s_2\rangle, \dots$, will occur at the fields $h_{s_0, s_1}, h_{s_1, s_2}, \dots$. We denote this cascade by $(s_0, s_1); (s_1, s_2); \dots$, and for each of its ground state changes the corresponding level-crossing fields $h_{s,s'}(d)$ is shown in Fig. 5. Generalizing CC's critical field to nonzero d , we denote the (parity-dependent) field at which the *first* transition (s_0, s_1) occurs by $h_{CC}(d, p) \equiv h_{s_0, s_1}(d)$, which simply is the lower envelope of the level-crossing fields h_{s_0, s_1} in Fig. 5. In the limit $d \rightarrow 0$ we find numerically that it correctly reduces to the Clogston-Chandrasekhar value $h_{CC}(0, p) = \tilde{\Delta}/\sqrt{2}$.

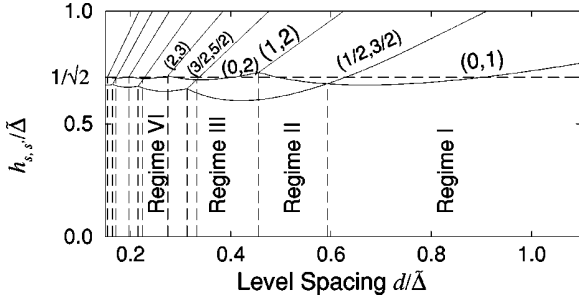


FIG. 5. The level-crossing fields $h_{s,s'}(d)/\bar{\Delta}$ [see Eq. (19)] for the cascade of ground state changes (GSCs) $(s_0, s_1); (s_1, s_2); \dots$, that occurs as h increases from 0 at given d . Some lines are labeled by the associated GSC (s, s') (where $\mathcal{E}_{s'}$ drops below \mathcal{E}_s as h increases past $h_{s,s'}$). (Level crossing fields *not* associated with a GSC are not shown.) The order in which GSCs can occur within a cascade (i.e., the order of $h_{s,s'}$ lines encountered when moving vertically upward in the figure) depends sensitively on d , and an infinite number of distinct regimes (cascades) I,II,III, \dots , can be distinguished. The lower curves show the first jump in the lowest line of a tunneling spectrum that occurs at the level-crossing field $h_{CC}(p, d) = h_{s_0, s_1}$. The size of this jump $|\Delta E_{s_1, f'} - \Delta E_{s_0, f}|$ differs for $e \rightarrow o$ (solid line) and $o \rightarrow e$ (dashed line) tunneling spectra but in both cases approaches the CC value $1 - 1/\sqrt{2} = 0.29$ as $d \rightarrow 0$. The nonmonotonic behavior is due to the discreteness of the level spacing.

In general, the order in which the GSC's occur with increasing h depends sensitively on d and an infinite number of distinct regimes (cascades) I,II,III, \dots , can be distinguished: Starting at large d we find the typical normal behavior $(0,1); (1,2); (2,3); \dots$, for even grains and $(\frac{1}{2}, \frac{3}{2}); (\frac{3}{2}, \frac{5}{2}); \dots$, for odd grains, with $h_{0,1} < (\text{or } >) h_{1/2, 3/2}$ in regimes I (or II). In regimes III and IV of somewhat smaller d , the order of GSC's is $(0,2); (2,3); \dots$, and $(\frac{1}{2}, \frac{3}{2}); (\frac{3}{2}, \frac{5}{2}); \dots$, etc., i.e., the spin s_1 attained after the first GSC (s_0, s_1) has increased to 2 in the even case. This illustrates a general trend: the spin $s_1(d)$ after the first transition increases with decreasing d and becomes macroscopically large in the $d \rightarrow 0$ limit, where $s_1 = h_{CC}/d = \bar{\Delta}/(d\sqrt{2})$, as explained in recounting CC's argument above.

Furthermore, it turns out that $\Delta_{s_1}(d) = 0$ for *all* d , implying that after the first GSC the new ground state $|s_1\rangle$ is *always* (not only in CC's bulk limit) an uncorrelated, purely paramagnetic state. In this regard, CC's picture of the transition remains valid throughout as d is increased: at $h_{CC}(d, p)$, a transition occurs from the superconducting ground state to a paramagnetic, uncorrelated state $|s_1\rangle_0$, the transition being first-order in the sense that $\Delta_{s_1}(d) = 0$; however, the first-order transition is "softened" with increasing d , in the sense that the size of the spin change $s_1 - s_0$ decreases from being macroscopically large in the bulk to being equal 1 at $d \gg \bar{\Delta}$ (regimes I and II).

F. Deficiencies of the variational ansatz

Though the variational method we used to calculate the systems "eigenenergies" is expected to yield qualitatively correct results, it does have some deficiencies. First, a variational approach by construction only gives an upper bound

on the exact eigenenergies $E_{s,\alpha}$. The variational energies $\mathcal{E}_{s,\alpha}$ could be lowered further by choosing better trial wave functions that sample larger parts of a given spin- s Hilbert space, i.e., by including "fluctuations" about the chosen states.

Secondly, the abrupt vanishing of the pairing parameters $\Delta_{s,\alpha}(d) \approx \sqrt{1 - d/d_{c,s}}$ at a critical level spacing $d_{c,s}$ [see Appendix and Fig. 3(a)] is unphysical: in a finite system, any nonzero pair-interaction constant will always induce a nonzero amount of pairing correlations, i.e., the canonical $\bar{\Delta}'_s(d)$ of Eq. (4) will always be nonzero, though it could become arbitrarily small for sufficiently large d . (This statement is analogous to stating that "in a finite system no abrupt phase transition between a zero and nonzero order parameter occurs.") The abrupt, mean-field-like vanishing of $\Delta_{s,\alpha}(d)$ is of course an artifact, that occurs since the grand-canonical variational *Ansatz* is equivalent (at least for the spin- s ground states $|s\rangle$) to doing mean-field theory in a fixed- s Hilbert space.

Thirdly, the variational states of course are not \hat{N} eigenstates (though they do have definite parity), and Eq. (13) only fixes the *mean* electron number. Our reasons for nevertheless adopting them to describe an isolated grain were given in Sec. II C: a large body of experience in nuclear physics showed that fixed- N projections generally produce only minor corrections to the grand-canonical BCS results. Nonetheless, note that we expect a fixed- N projection (currently under investigation²⁵) to somewhat ameliorate the first two of the abovementioned deficiencies of the variational approach: projection after variation of $|s\rangle$ to fixed N will lower the energy \mathcal{E}_s a bit, and presumably projection before variation will in addition result in a canonical pairing parameter $\bar{\Delta}_s(d)$ that decays smoothly with increasing d from finite to arbitrarily small but nonzero values. Note, though, that this is not expected to change the eigenenergies very much, since the correlation energies rapidly approach zero anyway when the correlations become weak. In other words, we expect the variational scheme for calculating eigenenergies to break down only when Δ_s becomes so small that it has no experimental relevance any more (to check this in detail, strictly canonical calculations are needed^{25,27}).

IV. OBSERVABLE QUANTITIES

In this section, we consider the grain coupled to leads as in RBT's SET experiments. After explaining what kind of information can and can not be extracted from their data, we turn to the calculation of observable quantities. (a) We calculate theoretical tunneling spectra and compare these to RBT's measurements and (b) *address the question of the observability of various parity effects, proposing to search for one involving the pair-breaking energy.*

A. Experimental details

In RBT's experiments,^{6,7,9} an ultrasmall grain was used as central island in a SET: it was connected via tunnel barriers to external leads and capacitively coupled to a gate, and its electronic spectrum determined by measuring the tunnel current through the grain as a function of transport voltage (V),

gate voltage (V_g) and magnetic field ($H=h/\mu_B$, with $\mu_B=0.0571$ meV/T) at a fixed temperature of 50 mK.

The particular grain [Ref. 9, Figs. 1(b),2,3] with which we shall compare our theory had the following parameters: Its radius was estimated as $r\approx 4.5$ nm by assuming the grain to be hemispherical, implying a volume $\approx (5.7 \text{ nm})^3$ and a total number of conduction electrons N of about 3×10^4 . The crude order-of-magnitude free-electron estimate $d=2\pi^2\hbar^2/(mk_F\text{Vol})$ for the mean level spacing near ε_F yields $d\approx 0.45$ meV. The SET had lead-to-grain capacitances $C_1=3.5$ aF, $C_2=9.4$ aF, gate-to-grain capacitance $C_g=0.09$ aF, and charging energy $E_C=e^2/2C_{\text{total}}=46$ meV. The tunnel current is on the order of 10^{-10} A, implying an average time of 2×10^{-9} sec between subsequent tunneling processes.

Since the charging energy E_C was very much larger than all other energy scales, such as the bulk gap ($\tilde{\Delta}\approx 0.38$ meV), typical values of the transport voltage ($V\lesssim 1$ mV) and the temperature, fluctuations in electron number on the grain are strongly suppressed, so that coherent superpositions between states with different N need not be considered. The energy-balance condition that determines through which eigenstates of the grain electrons can tunnel for given values of transport and gate voltage thus involve differences between the eigenenergies of a grain with fixed particle number N or $N\pm 1$,

$$\Delta E_{if}\equiv(E_f^N+E_C^N)-(E_i^{N\pm 1}+E_C^{N\pm 1}), \quad (20)$$

corresponding to the energy cost needed for some rate-limiting electron tunneling process $|i\rangle_{N\pm 1}\rightarrow|f\rangle_N$ off or onto the grain. Here $|f\rangle_N$ denotes a discrete eigenstate of the N -electron grain with eigenenergy $E_f^N+E_C^N$. Following the ‘‘orthodox model’’ of SET charging, we take E_C^N , the grain’s electrostatic energy (relative to a neutral grain with N_0 electrons) as $E_C^N=E_C(N-N_0-Q_g/e)^2$, where $Q_g=C_g V_g + \text{const}$ is the gate charge, and assume the Coulomb-interaction to be screened sufficiently well that its sole effect is to shift *all* fixed- N eigenstates by the same constant amount E_C^N . (The latter assumption is somewhat precarious: it becomes worse with decreasing grain size, and was shown to break down in grains half the present size.¹⁰)

RBT were able to extract the energy differences ΔE_{if} from their data: the differential conductance dI/dV as function of V at fixed V_g has a peak whenever eV times a known capacitance ratio is equal to one of the ΔE_{if} ’s, at which point another channel for carrying tunneling current through the grain opens up (the inclusion of the capacitance ratio takes into account that the voltage drop across each of the two tunnel junctions can be different if their capacitances are not identical⁹). Plotting the position of each conductance peak as function of h gives the so-called experimental tunneling spectrum shown in Fig. 6, in which each line reflects the H dependence of one of the energy differences $\Delta E(h)$.

It is important to note that the experimental threshold energy at $h=0$ for the lowest-energy tunneling process (y intercept of the lowest line, the so-called ‘‘tunneling threshold’’) yields no significant information, since it depends on the grain’s change in overall charging energy due to tunneling,

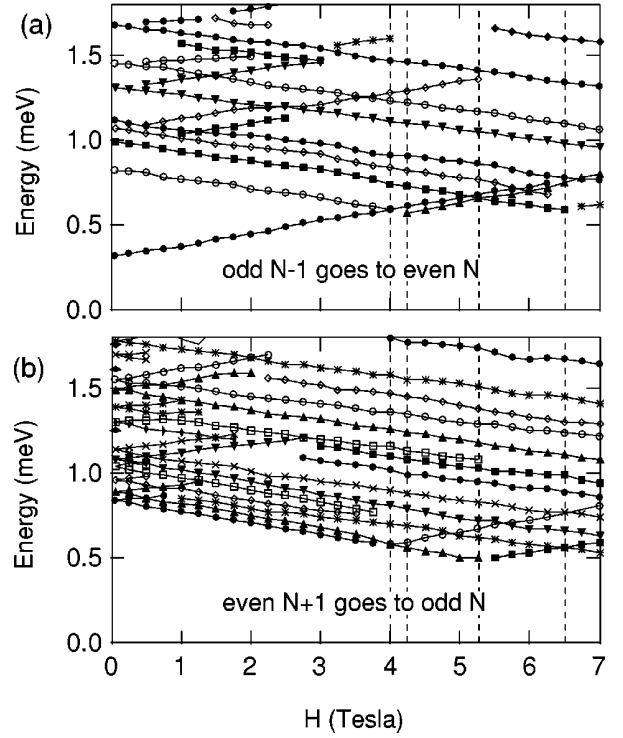


FIG. 6. Experimental tunneling spectra measured by RBT (Fig. 3 of Ref. 9). The distances between lines give the fixed- N excitation spectra of (a) an even and (b) an odd grain, as explained in Sec. IV A. The vertical dashed lines indicate the first four level-crossing fields $H_{s,s'}$ (assigned by comparison with Fig. 7, see Sec. IV B), namely $H_{0,1}=4T$, $H_{1/2,3/2}=4.25T$, $H_{1,2}=5.25T$, and $H_{3/2,5/2}=6.5T$ with uncertainty $\pm 0.13T$ (half the H resolution of $0.25T$).

$$\delta E_C=E_C^N-E_C^{N\pm 1}=E_C\left[Q_g/e-\left(N-N_0\pm\frac{1}{2}\right)\right], \quad (21)$$

which depends (via Q_g) in an imprecisely known way on the adjustable gate voltage V_g . This V_g dependence can usually (e.g., in SET’s with much smaller charging energies than here) be quantified precisely by studying the Coulomb oscillations that occur as function of V_g at fixed V . Unfortunately, in the present case a complication arises²⁴ due to the smallness of the gate capacitance: to sweep Q_g through one period of $2e$, the gate voltage V_g must be swept through a range so large ($2e/C_g\approx 3.5$ V) that during the sweep, RBT routinely observed small ‘‘rigid’’ shifts of the entire tunneling spectrum at random values of V_g . They presumably are due to single-electron changes in the charge contained in other metal grains in the neighborhood of the grain of interest; these changes produce sudden shifts in the electrostatic potential of the grain, and thus spoil the exact $2e$ periodicity that would otherwise have been expected for the spectra.

In contrast to the threshold energy, however, the separations between lines,

$$\Delta E_{if'}-\Delta E_{if}=E_{f'}^N-E_f^N, \quad (22)$$

are independent of gate voltage and hence known absolutely; they simply correspond to the differences between eigenen-

ergies of a *fixed-N* grain, i.e., give its fixed-*N* excitation spectrum, and these are the quantities that we shall focus on calculating below.

The most notable feature of RBT's measured tunneling spectra is the presence (absence) of a clear spectroscopic gap $2\Omega_e > d$ between the lowest two lines of the odd-to-even (even-to-odd) measured spectra in Figs. 6(a) and 6(b). This reveals the presence of pairing correlations: in even grains, all excited states involve at least two BCS quasiparticles and hence lie significantly above the ground state, whereas odd grains *always* have at least one quasiparticle and excitations need not overcome an extra gap.

Since the ΔE_{if} 's in Eq. (20) are constructed from *fixed-N* and *fixed-N* ± 1 eigenenergies, we shall approximate these using the variational energies $\mathcal{E}_{s\alpha}$ discussed in previous sections for a completely *isolated* grain. (We thereby make the implicit assumption that the grain's coupling to the leads is sufficiently weak that this does not affect its eigenenergies, i.e., that the leads act as "ideal" probes of the grain.) The $\mathcal{E}_{s\alpha}$ will be used as a starting point to discuss various observable quantities; in particular, we shall make contact with RBT's experimental results by constructing the theoretical tunnel spectrum (as function of *h* and *d*) predicted by our model.

B. The tunneling spectrum in a magnetic field

The kind of tunneling spectrum that results depends in a distinct way on the specific choice of level spacing *d* and final-state parity *p* (i.e., the parity of the grain after the rate-limiting tunneling process has occurred). To calculate the spectrum for given *d* and *p*, we proceed as follows below: we first analyze at each magnetic field *h* which tunneling processes $|i\rangle_{N\pm 1} \rightarrow |f\rangle_N$ are possible, then calculate the corresponding energy costs $\Delta E_{if}(h)$ of Eq. (20) and plot $\Delta E_{if}(h) - \Delta E_{\min}(0)$ as functions of *h* for various combinations of *i, f*, each of which gives a line in the spectrum. We subtract $\Delta E_{\min}(0)$, the *h*=0 threshold energy cost for the lowest-lying transition, since in experiment it depends on V_g and hence yields no significant information, as explained above. Figure 7 shows four typical examples of such theoretical tunneling spectra, with some lines labeled by the corresponding $|i\rangle \rightarrow |f\rangle$ transition.

When taking the data for Fig. 6, RBT took care to adjust the gate voltage V_g such as to minimize nonequilibrium effects, which we shall therefore neglect. For given *h*, we thus consider only those tunneling processes for which the initial state $|i\rangle$ corresponds to the grain's ground state $|s_i\rangle$ at that *h* (and *d, p*), whose spin s_i can be inferred from Fig. 5. Since the grain's large charging energy ensures that only one electron can tunnel at a time, the set $\{|f\rangle\}$ of possible final states satisfies the "spin selection rule" $|s_f - s_i| = \frac{1}{2}$ and includes, besides the spin- s_f ground state $|s_f\rangle$, also excited spin- s_f states.

Whenever *h* passes through one of the level-crossing fields $h_{s_i, s_{i'}}$ of Eq. (19), the grain experiences a ground state change $(s_i, s_{i'})$. After this GSC, $|s_{i'}\rangle$ is the new initial state for a new set of allowed tunneling transitions $|s_{i'}\rangle \rightarrow \{|s_{f'}\rangle\}$ (satisfying $|s_{f'} - s_{i'}| = 1/2$). Since this new set in general differs from the previous set of transitions $|s_i\rangle \rightarrow \{|f\rangle\}$ allowed before the GSC, at $h_{s_i, s_{i'}}$ one set of lines in the tunneling

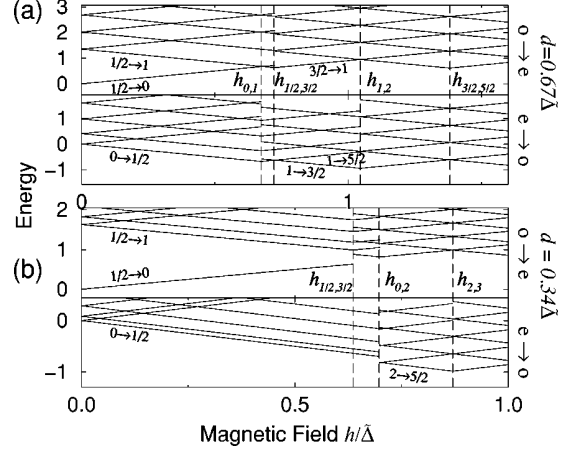


FIG. 7. The theoretical odd-to-even and even-to-odd tunneling spectra $[\Delta E_{if} - \Delta E_{\min}(0)]/\bar{\Delta}$ predicted for an ultrasmall superconducting grain as a function of magnetic field *h*, for two different level spacings: (a) $d = 0.67\bar{\Delta}$ and (b) $d = 0.34\bar{\Delta}$ (corresponding to regimes I and III of Fig. 5, respectively). Some lines are labeled by the corresponding $s_i \rightarrow s_{i'}$ tunneling transition. Not all possible higher lines (corresponding to excited final states $|s_{i'}\rangle$) are shown. Vertical dashed lines indicate those level-crossing fields $h_{s_i, s_{i'}}$ [see Eq. (19)] at which kinks or jumps occur, with $h_{0,1} < h_{1/2,3/2} < h_{1,2} < h_{3/2,5/2}$ in (a) and $h_{1/2,3/2} < h_{0,2} < h_{2,3}$ in (b).

spectrum ends and another begins. A line from the former connects continuously to one from the latter only if its final state $|f\rangle$ can be reached from both $|s_i\rangle$ and $|s_{i'}\rangle$ [i.e., if $s_f - s_i = -(s_f - s_{i'})$]; in this case, the two lines $|s_i\rangle \rightarrow |f\rangle$ and $|s_{i'}\rangle \rightarrow |f\rangle$ join at $h_{s_i, s_{i'}}$ via a kink, since $\Delta E_{if}(h)$ and $\Delta E_{i'f}(h)$ have slopes of opposite sign. However, for most lines this is not the case (since usually $|s_f - s_{i'}| \neq 1/2$), so that at $h_{s_i, s_{i'}}$ the line $|s_i\rangle \rightarrow |f\rangle$ simply ends while new lines $|s_{i'}\rangle \rightarrow |f'\rangle$ begin. This results in discontinuities (or "jumps") in the spectrum at $h_{s_i, s_{i'}}$ of size $(\Delta E_{i'f'} - \Delta E_{if})(h_{s_i, s_{i'}})$, unless by chance some other final state $|f'\rangle$ happens to exist for which this difference equals zero.

Since the order in which the GSC's $(s_i, s_{i'})$ occur as functions of increasing *h* depend on *d* and *p*, as indicated by the distinct regimes I, II, III, ..., in Fig. 5, one finds a distinct kind of tunneling spectrum for each regime, differing from the others in the positions of its jumps and kinks. In regime I, where the order of occurrence of GSC's with increasing *h* is $(0,1); (\frac{1}{2}, \frac{3}{2}); (1,2); (\frac{3}{2}, \frac{5}{2}); \dots$, there are no discontinuities in the evolution of the lowest line [see Fig. 7(a)]. For example, for the $e \rightarrow o$ spectrum, the lowest $|0\rangle \rightarrow |1/2\rangle$ line changes *continuously* to $|1\rangle \rightarrow |1/2\rangle$ at $h_{0,1}$, since $|s_f - s_{i'}| = 1/2$. However, in all other regimes the first change in ground state spin (at h_{0, s_1} from 0 to s_1) is > 1 , implying a *jump* (though possibly small) in all $e \rightarrow o$ lines, as illustrated by Fig. 7(b).

The jump's magnitude for the tunneling thresholds, i.e., the lowest $e \rightarrow o$ and $o \rightarrow e$ lines, is shown as function of *d* in the lower part of Fig. 5. It starts at $d=0$ from the CC value $\bar{\Delta}(1 - 1/\sqrt{2})$ measured for thin Al films,²¹ and with increasing *d* decreases to 0 (nonmonotonically, due to the discrete spectrum). This *decrease of the size of the jump in the tun-*

neling threshold reflects the fact, discussed in Sec. III E, that the change in spin at the first ground state change (s_0, s_1) decreases with increasing d (as $s_1 - s_0 \sim h_{CC}/d$), and signals the softening of the first-order superconducting-to-paramagnetic transition.

The fact that the measured tunneling thresholds in Fig. 6 show no jumps at all (which might at first seem surprising when contrasted to the threshold jumps seen at h_{CC} in thin films in a parallel field²⁹), can therefore naturally be explained¹⁵ by assuming the grain to lie in the “minimal superconductivity” regime I of Fig. 5 (where the jump size predicted in Fig. 5 is zero). Indeed, the overall evolution (i.e., order and position of kinks, etc.) of the lowest lines of Fig. 6 qualitatively agrees with those of a regime I tunneling spectrum, Fig. 7(a). This allows us to deduce the following values for the level-crossing fields H_{s_i, s'_i} (indicated by vertical dashed lines in Figs. 6 and 7): $H_{0,1}=4T$, $H_{1/2,3/2}=4.25T$, $H_{1,2}=5.25T$, and $H_{3/2,5/2}=6.5T$. As corresponding uncertainties we take $\Delta H_{s_i, s'_i}=0.13T$, which is half the H resolution of $0.25T$ used in experiment.

By combining the above H_{s_i, s'_i} values with Fig. 5, some of the grain’s less-well-known parameters can be determined somewhat more precisely: First, the grain’s “bulk H_{CC} ” field can be estimated by noting from Fig. 5 that $h_{0,1}/h_{CC} \approx 0.95$, so that $H_{CC}=H_{0,1}/0.95 \approx 4.2T$. This is in rough agreement with the value $H_{CC} \approx 4.7T$ found experimentally²¹ in thin films in a parallel field, confirming our expectation that these correspond to the “bulk limit” of ultrasmall grains as far as paramagnetism is concerned. (Recall that our numerical choice of $\lambda=0.194$ in Sec. III D was based on this correspondence.) Secondly, the grain’s corresponding bulk gap is $\tilde{\Delta} = \sqrt{2}\mu_B H_{CC} \approx 0.34$ meV. Thirdly, to estimate the level spacing d , note that since $H_{1/2,3/2}/H_{0,1} \approx 1.06$, this grain lies just to the right of the boundary between regions II and I in Fig. 5 where $d/\tilde{\Delta} \approx 0.63$, i.e., $d \approx 0.21$ meV. (The crude volume-based value $d \approx 0.45$ meV of Sec. IV A thus seems to have been an overestimate.) It would be useful if the above determination of d could be checked via an independent accurate experimental determination of d directly from the spacing of lines in the tunnel spectrum; unfortunately, this is not possible: the measured levels are shifted together by interactions, implying that their spacing does not reflect the mean *independent-electron* level spacing d .

The higher lines plotted in Fig. 7 correspond to states where the electron tunnels into an excited spin- s_f state. For simplicity we considered only excited states $|s_f, j\rangle$ involving a single electron-hole excitation relative to $|s_f\rangle$, such as the example discussed in Sec. III D 2 or as sketched in Fig. 2(b), though in general others are expected to occur too. The jumps in these lines [e.g., in Fig. 7(a) at $h_{1,2}$] occur whenever the two final excited states $|s_f, j_f\rangle$ and $|s_{f'}, j_{f'}\rangle$ before and after the GSC at h_{s_i, s'_i} have different correlation energies. (Recall that the correlation energy of an excited state $|s_f, \alpha_f\rangle$ can be nonzero even if that of the corresponding ground state $|s_f\rangle$ is zero, since the former’s unpaired electrons are further away from ϵ_F , so that $\Delta_{s_f, \alpha_f} > \Delta_{s_f}$, see Sec. III D 2.) Experimentally, these jumps have not been observed. This may be because up-moving resonances lose am-

plitude and are difficult to follow⁹ with increasing h , or because the widths of the excited resonances ($\approx 0.13\tilde{\Delta}$) limit energy resolution.¹⁰

For somewhat larger grains, the present theory predicts jumps even in the lowest line. It remains to be investigated, though, whether orbital effects, which rapidly increase with the grain size, would not smooth out such jumps.

Finally, note that more than qualitative agreement between theory and experiment can not be expected: in addition to the caveats mentioned in the second paragraph of Sec. III D, we furthermore neglected nonequilibrium effects in the tunneling process and assumed equal tunneling matrix elements for all processes. In reality, though, random variations of tunneling matrix elements could suppress some tunneling processes which would otherwise be expected theoretically.

C. Parity effects

As mentioned in the Introduction, several authors^{12–15} have discussed the occurrence of a parity effect in ultrasmall grains: “superconductivity” (more precisely, ground state pairing correlations) disappears sooner with decreasing grain size in an odd than an even grain ($\Delta_{1/2} < \Delta_0$, and $d_{c,1/2} < d_{c,0}$). This is a consequence of the blocking effect, which is always stronger in the presence of an odd, unpaired electron than without it. This section is devoted to discussing to what extent this and related parity effects are measurable. Since pairing parameters such as $\Delta_{1/2}, \Delta_0$ are not observable quantities, measurable consequences of parity effects must be sought in differences between eigenenergies, which in principle are measurable.

1. In ultrasmall grains, $E_{1/2} - E_0$ is currently not measurable

One might expect that the odd-even ground state energy difference $E_G^{ole} \equiv (E_{1/2} - E_0)$ should reveal traces of the parity effect. Regrettably, *in ultrasmall grains this quantity not directly measurable in the current generation of experiments* by RBT, for the following reasons.

If the transport voltage V is varied at fixed gate voltage V_g , the energy cost of changing the grain’s electron number by 1 (the $h=0$ threshold tunneling energy) depends [see Eq. (20)] not only on E_G^{ole} but also on the change δE_C in the grain’s charging energy due to tunneling. However, as explained in Sec. IV A, δE_C depends (in an imprecisely known way) on the actual value of V_g . Therefore only the grain’s fixed- N excitation spectrum (distance between lines of tunneling spectrum) can be measured accurately in this way, but not E_G^{ole} .

If the gate voltage V_g is varied at a fixed transport voltage in the linear response regime $V \approx 0$, i.e., Coulomb oscillations are studied, one expects to find a $2e$ periodicity in the so-called gate charge $Q_g = C_g V_g + \text{const}$, with E_G^{ole} determining the amount of deviation from the e periodicity (see Appendix B for details). Analyzing these deviations thus in principle allows one to experimentally determine E_G^{ole} , as has been demonstrated convincingly in μm -scale devices.^{32,33}

However, the parity effects discussed in the present paper are only expected to occur in devices very much smaller than those of Refs. 32 and 33, namely, in nm-scale devices such

as those of RBT. Regrettably, for these it is at present not possible to study (as suggested in Ref. 14) e - or $2e$ -dependent features with sufficient accuracy to carry through the procedure described above: due to the extremely small size of nm-scale grains, their charging energy is so large that the predicted pairing-induced deviation from e periodicity is a very small effect (a fractional change of order $E_G^{o/e}/E_C < 0.01$). Moreover, even if observable in principle, in present experiments this small effect would be obscured by deviations from periodicity of a different origin: as explained in Sec. IV A, RBT routinely observed sudden V_g -dependent shifts in background charge²⁴ near the transistor when they sweep V_g through the large range necessary to cover more than one period, and according to RBT,²⁴ the resulting random deviations from periodicity make it impossible to analyze e vs $2e$ effects with the accuracy required to extract $E_G^{o/e}$ -induced effects. Thus we conclude that at present $E_G^{o/e}$ is not directly measurable.

2. Parity effect in pair-breaking energies

Since the quantities that RBT can measure accurately are fixed- N excitation spectra, let us investigate what parity effects can be extracted from these. Since any parity effect is a consequence of the blocking effect, we begin by discussing the latter's most obvious manifestation: it is simply the fact that breaking a pair costs correlation energy, since the resulting two unpaired electrons disrupt pairing correlations. This, of course, is already incorporated in mean-field BCS theory via the excitation energy of at least $2\bar{\Delta}$ involved in creating two quasiparticles. It directly manifests itself in the qualitative difference between RBT's even and an odd excitation spectra (explained in Sec. IV A), namely, that the former shows a large spectral gap $2\Omega_e > d$ between its lowest two lines that is absent for the latter (Fig. 6).

The parity effect discussed by von Delft *et al.*¹² and Smith and Ambegaokar¹³ referred to a more subtle consequence of the blocking effect that goes beyond conventional BCS theory, namely, that the pairing parameters Δ_s have a significant s dependence once $d/\bar{\Delta}$ becomes sufficiently large. Although these authors only considered the ground state parity effect $\Delta_{1/2} < \Delta_0$, the same blocking physics will of course also be manifest in generalizations to $s > \frac{1}{2}$. In fact, the problems with measuring the odd-even ground state energy difference $E_G^{o/e}$ discussed above leave us no choice but to turn to $s > \frac{1}{2}$ cases when looking for a measurable parity effect. Specifically, we shall now show that a parity effect resulting from $\Delta_{3/2} < \Delta_1$ should in principle be observable in present experiments.

To this end, let us compare the $h=0$ pair-breaking energies in an even and an odd grain, defined as the energy per electron needed to break a single pair at $h=0$ by flipping a single spin: for an even grain, it is $\Omega_e \equiv \frac{1}{2}(E_1 - E_0)_{h=0}$, i.e., simply half the spectral gap discussed above; for an odd grain, it is $\Omega_o \equiv \frac{1}{2}(E_{3/2} - E_{1/2})_{h=0}$.

Within mean-field BCS theory, one would evaluate these using the same pairing parameter $\bar{\Delta}$ for all states and $[(\varepsilon_j - \mu_p)^2 + \bar{\Delta}^2]^{1/2}$ for the quasiparticle excitation energies associated with having the single-particle state $|j, \pm\rangle$ definitely occupied or empty, with parity-dependent chemical

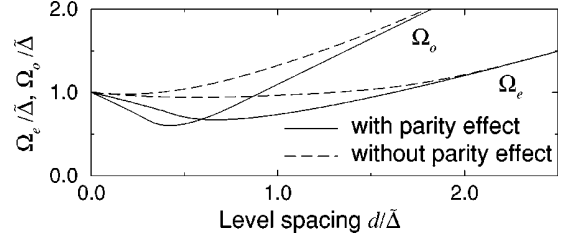


FIG. 8. Parity effect for the pair-breaking energies $\Omega_e \equiv \frac{1}{2}(E_1 - E_0)_{h=0}$ and $\Omega_o \equiv \frac{1}{2}(E_{3/2} - E_{1/2})_{h=0}$ (see Sec. IV C 2): when calculated naively using conventional mean-field theory (dashed lines), the pair-breaking energies obey $\Omega_o > \Omega_e$ for all $d/\bar{\Delta}$; in contrast, when calculated within generalized variational BCS theory (solid lines), $\Omega_o < \Omega_e$ for $d/\bar{\Delta} < 0.6$; this reflects a parity effect, namely that $\Delta_{3/2} < \Delta_1$, which is caused by the extra unpaired electron in $|3/2\rangle$ relative to $|1\rangle$.

potential¹² $\mu_p = \varepsilon_0 - pd/2$. This would give $\Omega_e^{\text{BCS}} = [(d/\bar{\Delta})^2 + \bar{\Delta}^2]^{1/2}$ and $\Omega_o^{\text{BCS}} = [d^2 + \bar{\Delta}^2]^{1/2}$, implying that the difference $\Omega_o^{\text{BCS}} - \Omega_e^{\text{BCS}}$ is strictly > 0 (Fig. 8, dotted lines). For $d/\bar{\Delta} \rightarrow \infty$ this difference reduces to d , which is simply the difference in the kinetic energy cost required to flip a single spin when turning $|\frac{1}{2}\rangle_0$ into $|\frac{3}{2}\rangle_0$ (namely, $2d$), relative to that when turning $|0\rangle_0$ into $|1\rangle_0$ (namely, d).

In contrast, using the present theory to go beyond mean-field BCS theory, one finds numerically that $\Omega_o > \Omega_e$ only for sufficiently large level spacings ($d/\bar{\Delta} > 0.6$, see Fig. 8, dotted lines); for smaller d one has $\Omega_o < \Omega_e$, implying that it costs less energy to break a pair in an odd grain than an even grain, even though the kinetic-energy cost is larger ($2d$ vs d). This happens since $\Delta_{3/2} < \Delta_1$, which reflects a parity effect caused by pair blocking by the extra unpaired electron in $|3/2\rangle$ relative to $|1\rangle$. *The theoretical result that $\Omega_o/\Omega_e < 1$ for sufficiently small $d/\bar{\Delta}$ can be viewed as a ‘‘pair-breaking energy parity effect’’ which is analogous to the ‘‘ground state parity effect’’ $\Delta_{1/2} < \Delta_0$, but which, in contrast to the latter, should be observable in the experimentally available fixed- N eigenspectra.*

What are Ω_e and Ω_o in RBT's experiments? Unfortunately, the present data do not give an unambiguous answer: on the one hand, the $h=0$ data allow the determination of $\Omega_e = 0.25$ meV [half the $h=0$ energy difference between the two lowest lines of Fig. 6(a)], but not of Ω_o , since breaking a pair is not the lowest-lying excitation of an odd system at $h=0$ [which is why Fig. 6(b) has no spectral gap]. On the other hand, both Ω_e and Ω_o can be found from $h \neq 0$ data, since by Eq. (19) they are equal to the level-crossing fields $h_{0,1} = \Omega_e$ and $h_{1/2,3/2} = \Omega_o$, whose values were deduced from the experimental tunneling spectra in Sec. IV B. This yields $\Omega_e = 0.23 \pm 0.01$ meV and $\Omega_o = 0.24 \pm 0.01$ meV, i.e., a Ω_e value somewhat *smaller* than the above-mentioned 0.25 meV determined at $h=0$. The reasons for this difference are presumably (i) that the actual g factors are not precisely 2 (as assumed), and (ii) that the experimental spectral lines are not perfectly linear in h (having a small h^2 contribution due to orbital diamagnetism, neglected in our model).

Nevertheless, if we assume that these two complications will not significantly affect the ratio $h_{1/2,3/2}/h_{0,1}$ (since $h_{1/2,3/2}$ and $h_{0,1}$ presumably are influenced by similar amounts), we

may use it to estimate the ratio $\Omega_o/\Omega_e = 4.25/4 = 1.06 \pm 0.1$. This ratio is slightly smaller than that expected from the mean-field BCS ratio $\Omega_o^{\text{BCS}}/\Omega_e^{\text{BCS}} \approx 1.1$ at $d/\tilde{\Delta} \approx 0.63$, i.e., consistent with the pair-breaking energy parity effect. However, the difference between 1.06 and 1.1 is probably too small to regard this effect as having been conclusively observed.

We suggest that it should be possible to conclusively observe the pair-breaking energy parity effect in a somewhat larger grain with $h_{1/2,3/2} < h_{0,1}$ (implying $\Omega_o/\Omega_e < 1$), i.e., in regime II of Fig. 5. (This suggestion assumes that in regime II the complicating effect of orbital diamagnetism is still nondominant, despite its increase with grain size.) To look for this effect experimentally would thus require good control of the ratio $d/\tilde{\Delta}$, i.e., grain size. We suggest that this might be achievable if a recently reported new fabrication method, which allows systematic control of grain sizes by using colloidal chemistry techniques,³⁴ could be applied to Al grains.

3. Parity effect in the limit $d/\tilde{\Delta} \gg 1$

Since the parity effects discussed above are based on the observation that the amount of pairing correlations, as measured by Δ_s , have a significant s dependence, they by definition vanish for $d > d_{c,0}$, because then $\Delta_s = 0$ for all s . Matveev and Larkin (ML) (Ref. 14) have pointed out, however, that there is a kind of parity effect that persists even in the limit $d/\tilde{\Delta} \gg 1$, which in the present theory we would call the ‘‘uncorrelated regime’’ [since there the $\tilde{\Delta}'$ defined in Eq. (4) would be $\ll \tilde{\Delta}$]: when one extra electron is added to an even grain, it does not participate at all in the pairing interaction, simply because this acts *only* between pairs; but when another electron is added so that now an extra pair is present relative to the initial even state, it does feel the pairing interaction and makes a self-interaction contribution $-\lambda d$ to the ground state energy. To characterize this effect, they introduced the pairing parameter

$$\Delta_p^{\text{ML}} = E_{1/2}^{N+1} - \frac{1}{2}(E_0^N + E_0^{N+2}), \quad (23)$$

with $N = \text{even}$. In first order perturbation theory in λ , i.e., using $E_{p/2}^{N+p} \equiv \langle p|H|p \rangle_0$ (where $|p \rangle_0$ is the uncorrelated Fermi ground state with $N+p$ electrons), one obtains $\Delta_p^{\text{ML,pert}} = \frac{1}{2}\lambda d$. This illustrates that this parity effect exists even in the complete absence of correlations, and increases with d .

Since our variational ground states $|p \rangle$ reduce to the uncorrelated Fermi states $|p \rangle_0$ when $\Delta_p = 0$, the above perturbative result for $d/\tilde{\Delta}$ can of course also be retrieved from our variational approach: we approximate E_0^N and $E_{1/2}^{N+1}$ by $\mathcal{E}_0(d)$ and $\mathcal{E}_{1/2}(d)$, respectively, both of which were calculated above, and E_0^{N+2} by $\mathcal{E}_0(d) - \lambda d$, since it differs from $\mathcal{E}_0(d)$ only by an extra electron pair at the band's bottom, whose interaction contribution in Eq. (8) is $-\lambda d(v_j^{(s)})^4$. Thus the variational result for ML's parity parameter is

$$\Delta_p^{\text{ML,var}} = \mathcal{E}_{1/2}(d) - \mathcal{E}_0(d) + \lambda d/2, \quad (24)$$

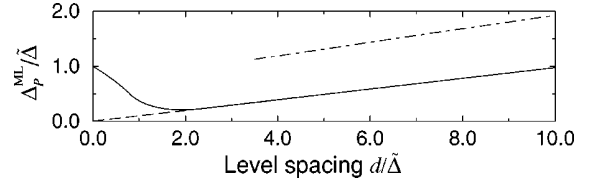


FIG. 9. The parity parameter Δ_p^{ML} discussed by Matveev and Larkin (Ref. 14), calculated perturbatively for the uncorrelated Fermi sea ($\Delta_p^{\text{ML,pert}} = \frac{1}{2}\lambda d$, dashed line), and using our generalized variational BCS approach [$\Delta_p^{\text{ML,var}}$ of Eq. (24), solid line]. The renormalized result $\Delta_p^{\text{ML}} \sim d/[2 \ln(ad/\tilde{\Delta})]$ given by ML is shown (dashed-dotted line) in its range of validity $d/\tilde{\Delta} \gg 1$. The parameter $a = 1.35$ is chosen to ensure quantitative agreement with exact diagonalization results for extremely small grains (Ref. 27).

(see Fig. 9), which reduces to the perturbative result $\Delta_p^{\text{ML,pert}}$ for $d > d_{c,0}$. The reason why this parity effect did not surface in the discussions of previous sections in spite of its linear increase with d is simply that there we were interested in correlation energies of the form $\mathcal{E} - \mathcal{E}^0$ in which effects associated with ‘‘uncorrelated’’ states were subtracted out [see, e.g., Figs. 3(b) and 4(b)].

The perturbative result $\Delta_p^{\text{ML,pert}} = \frac{1}{2}\lambda d$ is in a sense trivial. However, ML showed that a more careful calculation in the regime $d/\tilde{\Delta} \gg 1$ leads to a nontrivial upward renormalization $\tilde{\lambda}$ of the bare interaction constant λ , given with logarithmic accuracy by

$$\tilde{\lambda} \sim \frac{\lambda}{1 - \lambda \ln(\omega_c/d)}. \quad (25)$$

To obtain Δ_p^{ML} , λ in $\Delta_p^{\text{ML,pert}}$ is replaced by this renormalized $\tilde{\lambda}$, with the result

$$\Delta_p^{\text{ML}} \sim d/(2 \ln d/\tilde{\Delta}). \quad (26)$$

This logarithmic renormalization, which is beyond the reach of our variational method (but was confirmed using exact diagonalization in Ref. 27), can be regarded as the ‘‘first signs of pairing correlations’’ in what we in this paper have called the ‘‘uncorrelated regime’’ [in particular since $|\Delta_p^{\text{ML}}|$ increases upon renormalization only if the interaction is attractive, whereas it decreases for a repulsive interaction, see Eq. (25)]. Unfortunately, Δ_p^{ML} is at present not measurable, for the same experimental reasons as apply to E_G^{elo} , see Sec. IV C 1.

V. CONCLUSIONS

Citing the extensive literature in nuclear physics on fixed- N projections of BCS theory, we argued that a reasonable description of ultrasmall grains is possible using grand-canonical BCS theory, despite the fact that such grains would strictly speaking require a canonical description. Using a generalized variational approach to calculate various eigenenergies of the grain, we demonstrated the importance of the blocking effect (the reduction of pair-mixing correlations by unpaired electrons) and showed that it becomes stronger with decreasing grain size. The blocking effect is revealed in the magnetic-field dependence of the tunneling spectra of ultrasmall grains, in which pairing correlations can

be sufficiently weak that they are destroyed by flipping a single spin (implying ‘‘minimal superconductivity’’). Our theory qualitatively reproduces the behavior of the tunneling thresholds of the spectra measured by Ralph, Black, and Tinkham as a function of magnetic field. In particular, it explains why the first order transition from a superconducting to a paramagnetic ground state seen in thin films in a parallel field is softened by decreasing grain size. Finally, we argued that a pair-breaking energy parity effect (that is analogous to the presently unobservable ground state energy parity effect discussed previously) should be observable in experiments of the present kind, provided the grain size can be better controlled than in RBT’s experiments.

ACKNOWLEDGMENTS

We would like to thank I. Aleiner, B. Altshuler, V. Ambegaokar, S. Bahcall, C. Bruder, D. Golubev, B. Janko, K. Matveev, A. Rosch, A. Ruckenstein, G. Schön, R. Smith, and A. Zaikin for enlightening discussions. Special thanks go to D.C. Ralph and M. Tinkham for a fruitful collaboration in which they not only made their data available to us but also significantly contributed to the development of the theory. This research was supported by the German National Scholarship Foundation and the ‘‘SFB 195’’ of the Deutsche Forschungsgemeinschaft.

APPENDIX A: ANALYTICAL LIMITS

1. $d \rightarrow 0$ and Euler-MacLaurin expansion

When the level spacing d tends to zero the theory reduces to the conventional BCS variational and mean field approach. We can calculate the properties of a superconducting system to first order in d by expanding the BCS solution around $d=0$. In doing so, we focus on the ground states $|s\rangle$ of each spin- s sector of Hilbert space.

While in the bulk limit ($d=0$) the shift $-\lambda d(v_j^{(s)})^2$ in the single-electron energies ξ_j just after Eq. (12) is unimportant, it influences the behavior of an ultrasmall grain by effectively increasing the level-spacing near the Fermi surface. Its effect is largest for $s=0$, since for $s \neq 0$ the states at the Fermi surface, where the deviation of $v_j^{(s,\alpha)}$ from 0 or 1 is largest, are blocked. For simplicity we neglect the $v_j^{(s,\alpha)}$ dependence in ξ_j in the following calculation, using $\xi_j = \varepsilon_j - \mu - \lambda d \theta[-(\varepsilon_j - \mu)]$, and therefore good agreement with numerics can only be expected for $d \ll \tilde{\Delta}$ and $s \neq 0$. Within this approximation for ξ_j , μ lies halfway between the topmost double occupied and lowest completely empty level in $|s\rangle_0$: $\mu = \varepsilon_0 - d(\delta_{p,0} + \lambda)/2$. Note that μ does *not* lie exactly on one of the levels in the odd case ($p=1$) as one might have expected at first sight, but halfway between the topmost doubly occupied and lowest completely empty level.

We shall calculate the pairing parameter $\Delta_s(d)$ in the small- d limit by calculating the first terms of its Taylor series:

$$\Delta_s(d) = \left(1 + d\partial_d + \frac{d^2}{2}\partial_d^2\right)\Delta_s(0). \quad (\text{A1})$$

To this end, it suffices to solve the gap equation (12), as well its first and second derivatives with respect to d , for $d=0$.

This can be done by rewriting Eq. (12) using the Euler-MacLaurin summation formula

$$\begin{aligned} 1/\lambda = d \sum_{j=j_0}^{j_1} f(jd) &\simeq \int_{j_0 d}^{j_1 d} d\xi f(\xi) + \frac{d}{2}[f(j_0 d) + f(j_1 d)] \\ &+ \frac{d^2}{12}[f'(j_0 d) + f'(j_1 d)], \end{aligned} \quad (\text{A2})$$

with $f(jd) = [(jd)^2 + \Delta_s^2]^{-1/2}$, $j_0 = s + (1 + \lambda)/2$, and $j_1 = \omega_c/d$. The s dependence has now been absorbed in the lower bound j_0 of the sum. The negative branch of the sum is identical to the positive since μ lies halfway between the topmost doubly occupied and lowest completely empty level. It therefore suffices to calculate the positive branch times two. Setting $d=0$ in Eq. (A2) yields the well-known BCS bulk gap equation, whose solution is, by definition, $\Delta_s(0) = \tilde{\Delta}$. The first and second total derivatives with respect to d of Eq. (A2) yield $\partial_d \Delta_s(d=0) = -s$ and $\partial_d^2 \Delta_s(d=0) = -s^2/\tilde{\Delta}$, so that the desired result from Eq. (A1) is

$$\Delta_s(d) \simeq \tilde{\Delta} - (s + \lambda/2)d - \frac{(s + \lambda/2)^2 d^2}{2\tilde{\Delta}}. \quad (\text{A3})$$

We next calculate the eigenenergies \mathcal{E}_s by evaluating Eq. (8) up to first order in d , where the sums again are evaluated with the help of the Euler-MacLaurin formula. Since we are interested in the effects of pairing correlations we subtract the energy \mathcal{E}_p^0 of the uncorrelated Fermi sea $|p\rangle_0$:

$$\begin{aligned} (\text{even}) \quad \mathcal{E}_s - \mathcal{E}_0^0 &\simeq -\frac{\tilde{\Delta}^2}{2d} + \left(1 + \frac{\pi}{4}\right)\lambda\tilde{\Delta} + 2s\tilde{\Delta} \\ &- \left(s^2 - \frac{1}{12} + \frac{\pi+6}{4}\lambda s\right)d, \end{aligned} \quad (\text{A4a})$$

$$\begin{aligned} (\text{odd}) \quad \mathcal{E}_s - \mathcal{E}_{\frac{1}{2}}^0 &\simeq -\frac{\tilde{\Delta}^2}{2d} + \frac{\pi}{4}\lambda\tilde{\Delta} + 2s\tilde{\Delta} \\ &- \left(s^2 + \frac{1}{6} + \frac{\pi+6}{4}\lambda s + \frac{\lambda}{2}\right)d. \end{aligned} \quad (\text{A4b})$$

The d^{-1} term is the bulk correlation energy, which is slightly renormalized by the intensive $(1 + \pi/4)\lambda\tilde{\Delta}$ term, which in turn stems from the v^4 terms of Eq. (8). $2s\tilde{\Delta}$ is the bulk excitation energy for $2s$ quasiparticles. The d^1 term is the first-order correction for discrete level-spacing.

2. d near d_c and the small delta expansion

The other analytically tractable limit is $d \gg \Delta_s$, which holds for d near the critical spacing $d_{c,s}$ where Δ_s vanishes. First, we derive an expression for the critical $d_{c,s}$ by solving the gap equation with vanishing pairing parameter Δ_s for d :

$$\frac{1}{\lambda} = \sum_{j=j_0}^{\omega_c/d_{c,s}} \frac{1}{j} = \Psi(\omega_c/d_{c,s} + 1) - \Psi(j_0). \quad (\text{A5})$$

$\Psi(x)$ denotes the digamma function and j_0 equals $s + (1 + \lambda)/2$ again. Remembering that $\lambda = 1/\ln(2\omega_c/\bar{\Delta})$ and $\exp[\Psi(x)] \sim x^{-1/2}$ for large x this equation reduces to

$$\ln\left(\frac{2d_{c,s}}{\bar{\Delta}}\right) = -\Psi\left(s + \frac{1+\lambda}{2}\right) \quad (\text{A6})$$

$$d_{c,s} = \frac{\bar{\Delta}}{2} \exp\left[-\Psi\left(s + \frac{1+\lambda}{2}\right)\right]. \quad (\text{A7})$$

For $s \geq 1$ this can be simplified to

$$d_{c,s} \approx \frac{\bar{\Delta}}{2s + \lambda}. \quad (\text{A8})$$

Numerical values of $d_{c,s}/\bar{\Delta}$ ($\lambda = 0.194$) are 2.36, 0.77, 0.44, 0.31, \dots , for $s = 0, \frac{1}{2}, 1, \frac{3}{2}, \dots$, respectively. Near $d_{c,s}$ the pairing parameter vanishes as

$$\Delta_s \approx \bar{\Delta} \sqrt{1 - \frac{d}{d_{c,s}}} \quad \text{for } d \gg \Delta_s \text{ and } s > 0, \quad (\text{A9})$$

which we shall now show.

Since for the spin- s ground states with vanishing pairing parameter electron and hole pairs are symmetrically distributed around the Fermi surface, Eq. (13) again yields $\mu = \varepsilon_0 - d(\delta_{p,0} + \lambda/2)$. We turn to the gap equation (12). The spin dependence has been absorbed in j_0 . The positive and negative branches of the restricted sum are identical (because of the special symmetric value of μ), with $|\xi|$ ranging from $d[s + (1 + \lambda)/2] = dj_0$ to ω_c . It therefore suffices to calculate the positive branch times 2:

$$\frac{1}{\lambda} = \sum_{j=j_0}^{\omega_c/d} (j^2 + \Delta_s^2/d^2)^{-1/2} \approx \sum_{j=s+(1+\lambda)/2}^{\omega_c/d} \left(\frac{1}{j} - \frac{\Delta_s^2}{2d^2j^3}\right), \quad (\text{A10})$$

$$\sum_{j=s+(1+\lambda)/2}^{\omega_c/d_{c,s}} \frac{1}{j} \approx \sum_{j=s+(1+\lambda)/2}^{\omega_c/d} \left(\frac{1}{j} - \frac{\Delta_s^2}{2d^2j^3}\right).$$

To obtain Eq. (A10), the square root was expanded using $\Delta_s \ll d$. The remaining sums can be expressed by the polygamma functions $\Psi^{(n)}$ using the identity

$$\sum_{k=1}^n \frac{1}{k^m} = \zeta(m) - (-1)^m \frac{\Psi^{(m-1)}(n+1)}{(m-1)!}. \quad (\text{A11})$$

Replacing the sums by the polygamma functions and collecting terms leads to

$$\begin{aligned} & \Psi\left(\frac{\omega_c}{d_{c,s}} + 1\right) - \Psi\left(\frac{\omega_c}{d} + 1\right) \\ &= -\frac{\Delta_s^2}{4d^2} \left[\Psi''\left(\frac{\omega_c}{d} + 1\right) - \Psi''\left(s + \frac{1+\lambda}{2}\right) \right]. \end{aligned} \quad (\text{A12})$$

Now assume that d is close to $d_{c,s}$: $d = d_{c,s} - \delta d$ and $\delta d \ll d_{c,s}$. Expand the left hand side in δd and use the asymptotics for Ψ' (on the left hand side) and Ψ'' (on the right

hand side) for the large ω_c/d argument. Also the $\Psi''(s + \frac{1}{2})$ term is approximated by its asymptotic form $-s^{-2}$:

$$\frac{\delta d}{d_{c,s}} = -\frac{\Delta_s^2}{4d^2} \Psi''(s + \frac{1}{2}), \quad (\text{A13})$$

$$\Delta_s^2 = 4d^2 s^2 \frac{d_{c,s} - d}{d_{c,s}}, \quad (\text{A14})$$

$$\Delta_s = \bar{\Delta} \sqrt{1 - \frac{d}{d_{c,s}}}. \quad (\text{A15})$$

The last step was performed by remembering that $4d^2 s^2 = 4d_{c,s}^2 s^2 \approx \bar{\Delta}^2$ for $s \neq 0$.

Although Eq. (A9) was derived for d near $d_{c,s}$, it turns out to have a surprisingly large range of validity: its small- d expansion in powers of $d/\bar{\Delta}$ agrees (at least) up to second order with Eq. (A3), and for $s \geq 1$ it in fact excellently reproduces the numerical results for $\Delta_s(d)$ for *all* d . For $s = 0$ the asymptotic expansion of Ψ'' breaks down. Therefore directly from Eq. (A13) we deduce

$$\Delta_0 \approx \sqrt{\frac{4d^2}{12.1} \frac{d_{c,s} - d}{d_{c,s}}}, \quad (\text{A16})$$

where we used $\Psi''[(1 + \lambda)/2] \approx -12.1$. This result gives good agreement with numerics near $d_{c,s=0}$, but obviously has the wrong $d \rightarrow 0$ limit.

APPENDIX B: I - V CHARACTERISTICS OF AN ULTRASMALL NSN SET

In this appendix we discuss how the I - V characteristics of a SET in principle allow one to deduce even-odd ground state energy differences as mentioned in Sec. IV C 1. Tichy and von Delft³⁵ examined the I - V characteristics of a SET with an ultrasmall superconducting grain as island, i.e., an ultrasmall NSN SET. They described the discrete pair-correlated eigenstates of the grain using the parity-projected mean-field BCS theory of Ref. 12. Although this approach is too crude to correctly treat pairing correlations of excited states [since for all even (or odd) ones the *same* Δ_0 (or $\Delta_{1/2}$) is used], it does treat the even and odd ground states correctly. It therefore enables one to understand how the odd-even ground state energy difference $E_G^{o/e} \equiv (E_{1/2} - E_0)$ should influence the SET's I - V characteristics.

Using tunneling rates given by Fermi's golden rule and solving an appropriate master equation, Tichy calculated the tunnel current through the SET as a function of transport voltage V and gate voltage V_g at zero magnetic field. In an ideal sample, the I - V characteristics are $2e$ periodic in the gate charge $Q_g = V_g C_g + \text{const}$; one such period is shown in Fig. 10. The usual Coulomb-blockade "humps" centered roughly around the degeneracy points $Q_g/e = 2m \pm \frac{1}{2}$ are decorated by discrete steps, due to the grain's discrete eigenspectrum. In RBT's experiments V_g was fixed near a degeneracy point and the current measured as function of V

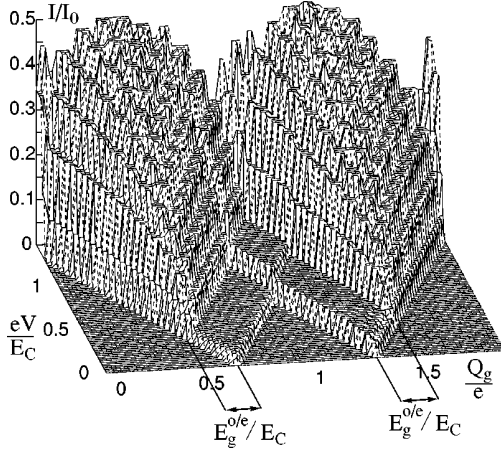


FIG. 10. I - V characteristics for a SET with an ultrasmall superconducting grain as island (from Ref. 35). The current is plotted as a function of gate charge (Q_g/e) and transport voltage (eV/E_C). Pairing correlations shift the degeneracy-point values of Q_g/e away from their e -periodic values of $2m \pm \frac{1}{2}$ by $\pm E_G^{ole}/E_C$ (see text). To better reveal the figure's characteristic features, it was plotted using a ratio $E_G^{ole}/E_C \approx 0.1$, very much larger than the typical values of < 0.01 .

(for a set of different H values). When following a line parallel to the V axis in Fig. 10, the positions of the steps in the current thus correspond to the $H=0$ eigenenergies of RBT's tunneling spectra in Fig. 6.

The reason for $2e$ instead of e periodicity are pairing correlations: First, the grain's odd-even ground state energy difference E_G^{ole} causes a shift in the degeneracy-point values for Q_g/e from $2m \pm \frac{1}{2}$ to $2m \pm (\frac{1}{2} + E_G^{ole}/E_C)$. Secondly, tunneling spectra measured in the V direction in Fig. 10 show a plateau after the first step if the final state after tunneling is even (i.e., for $\frac{1}{2} + E_G^{ole}/E_C \leq Q_g/e \leq \frac{3}{2} - E_G^{ole}/E_C$), but not if it is odd, corresponding to the presence or absence of a large spectral gap in the tunneling spectra of Figs. 6(a) or 6(b); this is due to the energy cost to break a pair, and the plateau's width is simply twice the even pair-breaking energy $2\Omega_e$ (see Sec. IV C 2).

By analyzing the derivation from e periodicity along the Q_g axis at $eV=0$, one can in principle experimentally determine E_G^{ole} . Unfortunately in present devices this is not possible in practice for reasons explained in Sec. IV C 1.

APPENDIX C: TIME REVERSAL SYMMETRY

When defining our model in Eq. (6), we adopted a *reduced* BCS Hamiltonian, in analogy to that conventionally used for macroscopic systems. In doing so, we neglected interaction terms of the form

$$-d \sum_{ijj'j'} \lambda(i,j,i',j') c_{i+}^\dagger c_{j-}^\dagger c_{i'-} c_{j'+} \quad (C1)$$

between non-time-reversed pairs $c_{i+}^\dagger c_{j-}^\dagger$, following Anderson's argument¹ that for a short-ranged interaction, the matrix elements involving time-reversed states $c_{j+}^\dagger c_{j-}^\dagger$ are much larger than all others, since their orbital wave functions interfere constructively.³⁶ Interestingly, the experimental re-

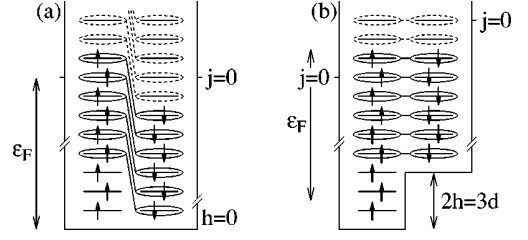


FIG. 11. Schematic representations of the non-time-reversed-pairing state $|3/2\rangle'$ defined in Eq. (C2). The energies $\varepsilon_{j,\mp} h$ of the single-particle states $|j, \pm\rangle$ are drawn (a) for $h=0$ and (b) for $2h=3d$. We indicated schematically how non-time-reversed states are paired according to $(u_i + v_i c_{i+3}^\dagger + c_{i-}^\dagger)$ in the BCS-like Ansatz (C2), with solid or dashed ellipses encircling states that would be completely filled or empty in the absence of pairing correlations.

sults of RBT provide strikingly direct support for the correctness of neglecting interactions between non-time-reversed pairs of the form (C1) at $h=0$: Suppose the opposite, namely, that the matrix elements $\lambda(j+k, j, j'+k, j')$ were all roughly equal to λ for a finite range of k values (instead of being negligible for $k \neq 0$, as assumed in H_{red}). Then for $2s < k$, one could construct a spin- s state $|s\rangle'$ with manifestly lower energy (\mathcal{E}') than that (\mathcal{E}) of the state $|s\rangle$ of Eq. (15):

$$|s\rangle' = \prod_{j=-m}^{-m+2s-1} c_{j+}^\dagger \prod_{i=-m}^{\infty} (u_i^{(s)} + v_i^{(s)} c_{i+2s}^\dagger + c_{i-}^\dagger) |\text{Vac}\rangle. \quad (C2)$$

Whereas in $|s\rangle$ pair mixing occurs only between time-reversed partners, in $|s\rangle'$ we have allowed pair mixing between *non*-time-reversed partners, while choosing the $2s$ unpaired spin-up electrons that occupy their levels with unit amplitude to sit at the band's *bottom* (see Fig. 11). To see that $|s\rangle'$ has lower energy than $|s\rangle$,

$$\mathcal{E}'_s = \mathcal{E}'_s^{\text{corr}} + \mathcal{E}'_s^0 < \mathcal{E}_s^{\text{corr}} + \mathcal{E}_s^0 = \mathcal{E}_s, \quad (C3)$$

we argue as follows: First, $\mathcal{E}'_s^0 = \mathcal{E}_s^0$, since the corresponding uncorrelated states $|s\rangle'_0$ and $|s\rangle_0$ are identical [and given by Eq. (16)]. Secondly, $\Delta'_s = \Delta_0 (> \Delta_s)$, and hence $\mathcal{E}'_s^{\text{corr}} = \mathcal{E}_0^{\text{corr}} (< \mathcal{E}_s^{\text{corr}} \leq 0)$, because the $2s$ unpaired electrons in $|s\rangle'$ sit at the band's bottom, i.e., so far away from ε_F that their blocking effect is negligible (whereas the $2s$ unpaired electrons in $|s\rangle$ sit around ε_F and cause significant blocking). Thus Eq. (C3) holds, implying that $|s\rangle'$ would be a better variational ground state for the interaction (C1) than $|s\rangle$.

Now, the fact that $\mathcal{E}'_s^{\text{corr}} = \mathcal{E}_0^{\text{corr}}$ is *independent* of s means that flipping spins in $|s\rangle'$ does not cost correlation energy. Thus, the energy cost for turning $|0\rangle'$ into $|1\rangle'$ by flipping one spin is simply the kinetic energy cost d , implying a threshold field $h'_{0,1} = d/2$ [see Eq. (19)]; in contrast, the cost for turning $|0\rangle$ into $|1\rangle$, namely, $2\Omega_e$, implies a threshold field $h_{0,1} = \Omega_e$, which (in the regime $d \lesssim \bar{\Delta}$) is rather larger

than $d/2$. The fact that RBT's experiments [Fig. 7(b)] clearly show a threshold field $h_{0,1}$ significantly larger than $d/2$ shows that the actual spin-1 ground state chosen by nature is better approximated by $|1\rangle$ than by $|1\rangle'$, in spite of the fact

that $\mathcal{E}'_1 < \mathcal{E}_1$. Thus the premise of the argument was wrong, and we can conclude that those terms in Eq. (C1) not contained in H_{red} can indeed be neglected, as done in the bulk of this paper.

-
- ¹P.W. Anderson, J. Phys. Chem. Solids **11**, 28 (1959).
²I. Giaever and H. R. Zeller, Phys. Rev. Lett. **20**, 1504 (1968).
³H. R. Zeller and I. Giaever, Phys. Rev. **181**, 789 (1969).
⁴M. Strongin, R. S. Thompson, O. F. Kammerer, and J. E. Crow, Phys. Rev. B **1**, 1078 (1970).
⁵B. Mühlischlegel, D.J. Scalapino, and R. Denton, Phys. Rev. B **6**, 1767 (1972).
⁶D. C. Ralph, C. T. Black, and M. Tinkham, Phys. Rev. Lett. **74**, 3241 (1995).
⁷C. T. Black, D. C. Ralph, and M. Tinkham, Phys. Rev. Lett. **76**, 688 (1996).
⁸D. C. Ralph, C. T. Black, and M. Tinkham, Physica B **218**, 258 (1996).
⁹D. C. Ralph, C. T. Black, and M. Tinkham, Phys. Rev. Lett. **78**, 4087 (1997).
¹⁰O. Agam, N. S. Wingreen, B. L. Altshuler, D. C. Ralph, and M. Tinkham, Phys. Rev. Lett. **78**, 1956 (1997).
¹¹O. Agam and I. L. Aleiner, Phys. Rev. B **56**, 5759 (1997).
¹²J. von Delft, A. D. Zaikin, D. S. Golubev, and W. Tichy, Phys. Rev. Lett. **77**, 3189 (1996).
¹³R. A. Smith and V. Ambegaokar, Phys. Rev. Lett. **77**, 4962 (1996).
¹⁴K. A. Matveev and A. I. Larkin, Phys. Rev. Lett. **78**, 3749 (1997).
¹⁵F. Braun, J. von Delft, D. C. Ralph, and M. Tinkham, Phys. Rev. Lett. **79**, 921 (1997).
¹⁶S. Bahcall (unpublished).
¹⁷B. Jankó, A. Smith, and V. Ambegaokar, Phys. Rev. B **50**, 1152 (1994).
¹⁸D. S. Golubev and A. D. Zaikin, Phys. Lett. A **195**, 380 (1994); *Quantum Dynamics of Submicron Structures*, edited by H. A. Cerdeira *et al.* (Kluwer, Dordrecht, 1995), p. 473.
¹⁹V. G. Soloviev, K. Dan. Vidensk. Selsk. Mat. Fys. Skr. **1**, 1 (1961).
²⁰Ya. M. Blanter (private communication).
²¹R. Meservey and P. M. Tedrow, Phys. Rep. **238**, 173 (1994).
²²P. Ring and P. Schuck, *The Nuclear Many-Body Problem* (Springer-Verlag, Berlin, 1980).
²³L. N. Cooper, J. Bardeen, and J. R. Schrieffer, Phys. Rev. **108**, 1175 (1957).
²⁴D. C. Ralph (private communication).
²⁵F. Braun and J. von Delft, Phys. Rev. Lett. **81**, 4712 (1998).
²⁶R. Balian, H. Flocard, and M. Veneroni, nucl-th/9706041, 1997 (unpublished).
²⁷A. Mastellone, G. Falci, and R. Fazio, Phys. Rev. Lett. **80**, 4542 (1998).
²⁸J. W. Garland, K. H. Bennemann, and F. M. Mueller, Phys. Rev. Lett. **21**, 1315 (1968).
²⁹R. Meservey, P. M. Tedrow, and Peter Fulde, Phys. Rev. Lett. **25**, 1270 (1970).
³⁰B. S. Chandrasekhar, Appl. Phys. Lett. **1**, 7 (1962).
³¹A. M. Clogston, Phys. Rev. Lett. **9**, 266 (1962).
³²M. T. Tuominen, J. M. Hergenrother, T. S. Tighe, and M. Tinkham, Phys. Rev. Lett. **69**, 1997 (1992); Phys. Rev. B **47**, 11 599 (1993); M. Tinkham, J. M. Hergenrother, and J. G. Lu, *ibid.* **51**, 12 649 (1996).
³³P. Lafarge, P. Joyez, D. Esteve, C. Urbina, and M.H. Devoret, Phys. Rev. Lett. **70**, 994 (1993).
³⁴D. L. Klein, R. Roth, A. K. L. Lim, A. P. Alivisatos, and Paul L. McEuen, Nature (London) **389**, 699 (1997).
³⁵Wolfgang Tichy, Diploma thesis, University of Karlsruhe, 1996.
³⁶Boris L. Altshuler (private communication).